

Jadeitites and Plate Tectonics

George E. Harlow,¹ Tatsuki Tsujimori,²
and Sorena S. Sorensen³

¹Department of Earth and Planetary Sciences, American Museum of Natural History, New York, NY 10024-5192; email: gharlow@amnh.org

²Pheasant Memorial Laboratory, Institute for Study of the Earth's Interior, Okayama University, Misasa, Tottori 682-0193, Japan; email: tatsukix@misasa.okayama-u.ac.jp

³Department of Mineral Sciences, Smithsonian Institution, Washington, DC 20013-7012; email: sorensen@si.edu

Annu. Rev. Earth Planet. Sci. 2015. 43:105–38

First published online as a Review in Advance on January 2, 2015

The *Annual Review of Earth and Planetary Sciences* is online at earth.annualreviews.org

This article's doi:
10.1146/annurev-earth-060614-105215

Copyright © 2015 by Annual Reviews.
All rights reserved

Keywords

high-pressure/low-temperature rocks, fluid-mediated transport, serpentinite mélange, subduction processes

Abstract

Jadeitite is a relatively rare, very tough rock composed predominantly of jadeite and typically found associated with tectonic blocks of high-pressure/low-temperature metabasaltic rocks (e.g., eclogite, blueschist) in exhumed serpentinite-matrix mélanges. Studies over the past ~20 years have interpreted jadeitite either as the direct hydrous fluid precipitate from subduction channel dewatering into the overlying mantle wedge or as the metasomatic replacement by such fluids of oceanic plagiogranite, graywacke, or metabasite along the channel margin. Thus, jadeitites directly sample and record fluid transport in the subduction factory and provide a window into this geochemical process that is critical to a major process in the Earth system. They record the remarkable transport of large ion lithophile elements, such as Li, Ba, Sr, and Pb, as well as elements generally considered more refractory, such as U, Th, Zr, and Hf. Jadeitite is also the precious form of jade, utilized since antiquity in the form of tools, adornments, and symbols of prestige.

Jadeitite: a rock composed primarily of clinopyroxene with jadeite content, typically from ~80 to 100 mol%; all jadeite jades are jadeitites

Jadeite jade: the form of jade composed principally (more than ~90%) of clinopyroxene of primarily jadeite composition ($\text{NaAlSi}_2\text{O}_6$)

Serpentinite: a rock composed principally of serpentine minerals (antigorite and/or lizardite) typically formed from the hydration of peridotite

Peridotite: a rock composed of >40% olivine and <10% plagioclase

Metasomatism: a chemical replacement of a rock or mineral by another, usually by fluid-mediated mass transfer

Ophiolite: a thrust sheet of rock sequence typical of an altered ocean floor—sediments, pillow basalts, gabbro, and ultramafic rock emplaced onto a continental margin via a plate tectonic collision

1. INTRODUCTION

Jadeite ($\text{NaAlSi}_2\text{O}_6$) was recognized early on as an anomaly among the sodium aluminosilicates in that it is much denser ($\sim 3.4 \text{ g/cm}^3$) than the others ($\sim 2.6 \text{ g/cm}^3$). It was reasonably assumed that high pressure must be responsible for the unusually high density of this mineral. The so-called jadeite problem was taken up almost simultaneously by Sobolev (1949, 1951) and Yoder (1950), and in a similar way for glaucophane by Miyashiro & Banno (1958). Yoder was not able to synthesize jadeite but appropriately analyzed the phase relationships between jadeite, analcime ($\text{NaAlSi}_2\text{O}_6 \cdot \text{H}_2\text{O}$), nepheline ($\text{NaAlSi}_3\text{O}_8$), albite ($\text{NaAlSi}_3\text{O}_8$), and quartz (SiO_2). Loring Coes Jr. did synthesize jadeite, in 1953 (see Roy & Tuttle 1956), but the experimental calibrations for the important reactions nepheline + albite = jadeite and albite = jadeite + quartz awaited the work of Robertson et al. (1957), Birch & LeComte (1960), and Newton & Kennedy (1968). Around this time, the new global paradigm of plate tectonics provided a mechanism for subjecting crustal rocks containing albite to suitably high pressure to form jadeite, namely the requirement that Earth's crust be recycled by subduction (e.g., Isacks et al. 1968, Ernst 1970). However, forming jadeite from feldspar in high-pressure metamorphism of graywacke, as in Sulawesi (formerly Celebes) (de Roever 1955), does not explain jadeite rock—jadeitite.

Known more commonly as jadeite jade, the rock, which is composed of >90% jadeite, has been revered for its extraordinary toughness as a tool stone even prior to Neolithic time. The most noteworthy occurrence is in the Kachin Hills of northern Myanmar (formerly Burma), the world's major source for this precious rock, where it is found in serpentinite boulder conglomerates and as veins and tectonic blocks in serpentinite. Although initially interpreted as an igneous intrusion into peridotite (e.g., Bleek 1908), a melt of jadeite composition defies any recognized model of melting on Earth. Thus, some other process, such as hydrothermal metasomatism of oceanic plagiogranite (trondhjemitic to dacitic igneous rocks with dominant albite and quartz), was suggested by Coleman (1961, 1980) in connection with jadeitite from California and expanded upon by Dobretsov (1984) in relationship to ophiolites (the term serpentinite mélanges should have been used, as discussed below) of the West Sayan, Khakassia, Russia, and the Polar Urals, Russia. In the intervening 30 years, great progress has been made in both the understanding and the discovery of jadeitite. The context of jadeitite as a fluid crystallization-to-metasomatic product in the context of the channel-wedge boundary of a fossil subduction system, exhumed in serpentinite-matrix mélange, is well established (e.g., Tsujimori & Harlow 2012, Harlow et al. 2014). Moreover, during this period, the number of described occurrences has expanded from around 8 to more than 16, with more likely on the way.

The purpose of this review is to present the context and contemporary understanding of jadeitites as hydrous fluid precipitates and metasomatic modifications generated by dewatering and dissolution in the subduction channel of subduction systems, terminated by some collisional tectonic event that exhumed the channel boundary as a serpentinite mélange. As a record of fluid-mediated transport along and through the channel boundary and of the tectonics of mélange exhumation, jadeitite and its associated lithologies are important to a fuller understanding of the subduction process and its relationship to arc volcanism via fluxing, to geochemical cycles, and to the Earth system. Some of the wording here derives from the recent review by Harlow et al. (2014). Mineral abbreviations throughout this review are mostly after Whitney & Evans (2010) and are summarized in **Table 1**.

2. JADEITITE AND JADE

The words jade and jadeite were originally synonymous, derived from the Spanish description of the ornamental and talismanic stone used by the Aztecs in what is now Mexico: *pedra de yjada* (stone

Table 1 Minerals, abbreviations, and formulae

Abbreviation	Mineral name	Formula	Notes
Ab	Albite	NaAlSi ₃ O ₈	Feldspar group
Ae	Aegirine	NaFe ³⁺ Si ₂ O ₆	A pyroxene component
Anl	Analcime	Ideally NaAlSi ₂ O ₆ •H ₂ O	—
Atg	Antigorite	Approximately Mg ₃ Si ₂ O ₅ (OH) ₄	Serpentine group; stable at higher temperatures
Brc	Brucite	Mg(OH) ₂	—
Chr	Chromite	FeCr ₂ O ₄	A spinel component
Chl	Chlorite	Clinochlore: Mg ₅ Al(AlSi ₃ O ₁₀)(OH) ₈ Chamosite: Fe ²⁺ ₅ Al(AlSi ₃ O ₁₀)(OH) ₈ Sudoite: Mg ₂ Al ₃ (AlSi ₃ O ₁₀)(OH) ₈	A mineral group; the most common components are listed
Cpx	Clinopyroxene	Generally NaM ³⁺ Si ₂ O ₆ –CaM ²⁺ Si ₂ O ₆	Pyroxenes with monoclinic crystal structure
Czo	Clinozoisite	Ca ₂ Al ₃ (SiO ₄) ₃ (OH)	Epidote group
Di	Diopside	CaMgSi ₂ O ₆	A pyroxene component
Ep	Epidote	Ca ₂ Fe ³⁺ Al ₂ (SiO ₄) ₃ (OH)	—
Gln	Glaucofane	Na ₂ (Mg ₃ Al ₂)Si ₈ O ₂₂ (OH) ₂	Amphibole group
Grs	Grossular	Ca ₃ Mg ₂ (SiO ₄) ₃	Garnet group
Grt	Garnet	M ²⁺ ₃ N ³⁺ ₂ (SiO ₄) ₃	Generic silicate garnet
Hd	Hedenburgite	CaFeSi ₂ O ₆	A pyroxene component
Jd	Jadeite	NaAlSi ₂ O ₆	A pyroxene component
Ktp	Katophorite	Na(CaNa)(Mg ₄ Al)AlSi ₇ O ₂₂ (OH) ₂	Amphibole group
Ky	Kyanite	AlSi ₂ O ₅	High-pressure polymorph
Lz	Lizardite	Mg ₃ Si ₂ O ₅ (OH) ₄	Serpentine group; stable at lower temperatures
Lws	Lawsonite	CaAl ₂ Si ₂ O ₇ (OH) ₂ •H ₂ O	—
Ms	Muscovite	KAl(AlSi ₃ O ₁₀)(OH) ₂	Mica group
Ne	Nepheline	(Na,K)AlSiO ₄	—
Ol	Olivine	(Mg,Fe) ₂ SiO ₄	—
Omp	Omphacite	Ideally (CaNa)[(Mg,Fe)Al](Si ₂ O ₆) ₂	Pyroxene group
Opx	Orthopyroxene	(Mg,Fe)SiO ₃	—
Pg	Paragonite	NaAl ₂ (AlSi ₃ O ₁₀)(OH) ₂	Mica group
Ph	Phengite	KAl ₂ (AlSi ₃ O ₁₀)(OH) ₂	A varietal of muscovite, formed at high pressure, in which there is a considerable, perhaps 10%, Tschermaks exchange: Mg + Si for ^{vi} Al + ^{iv} Al (superscripts denote coordination number in the crystal structure)
Pmp	Pumpellyite-(Mg)	Ca ₂ MgAl ₂ (Si ₃ O ₁₁)(OH) ₂ •H ₂ O	Most common; -(Fe ²⁺), -(Fe ³⁺), and -(Mn) species also occur
Qz	Quartz	SiO ₂	—
Rt	Rutile	TiO ₂	—
Tr	Tremolite	Ca ₂ (Mg,Fe) ₅ Si ₈ O ₂₂ (OH) ₂	—
Ttn	Titanite	CaTiSiO ₅	Also known as sphene
Zrn	Zircon	ZrSiO ₄	—

Mélange: from French; a lithological unit of mixed rock types as blocks in a highly deformed fine-grained matrix, formed along a fault, typically at the upper boundary of a subduction channel

Jade: the term used in Western cultures for two monomineralic rocks, jadeite and nephrite, that have extreme fracture toughness and are used for fashioning tools and ornaments

Nephrite: the form of jade composed principally of a microcrystalline intergrowth of felted amphibole grains, primarily of tremolite [$\text{Ca}_2(\text{Mg,Fe})_5\text{Si}_8\text{O}_{22}(\text{OH})_2$] composition

Porphyroblasts: larger grains of a mineral within a generally finer-grained metamorphic rock

of the side or loins), worn to ease pain in the side or stomach (see Foshag 1957, Mottana 2012). *Jade* was a mistranslation into French (Buffon 1749, 1783–1788) that persists to this day. The essence of this New World stone was later determined to be the mineral jadeite (Damour 1881), but by that time it had already been confused with the green stone most familiar from China, Werner's *lapis nephriticus* or nephrite [the massive form of tremolite, $\text{Ca}_2(\text{Mg,Fe})_5\text{Si}_8\text{O}_{22}(\text{OH})_2$; Damour 1846]. Both forms of jade were revered as tool stones because of their toughness and suitability for fashioning axes (celts), chopping stones, and hammers, certifiably during the Neolithic but probably as early as the Paleolithic (before 35000 BCE). Subsequently, the more attractive colored versions of jade were transformed into talismanic and artistic forms to convey well-being, power, and status. A jade culture existed in a variety of places but was retained only in Southeast Asia, although the stone is now appreciated more widely via archaeology and artistic culture (**Figure 1**).

Nonetheless, there is an important geological connection to the archaeological legacy: Jade objects were known prior to the modern knowledge of their sources. This connection has aided the discovery and recognition of new sources of jadeite. Maya jadeite jade was recognized long before the identification of the source area along the Motagua River of Guatemala (Foshag & Leslie 1955, McBirney et al. 1967). Our own work later greatly magnified the footprint of Guatemalan jadeite and its context (Harlow 1994, Harlow et al. 2011, and citations therein). The recognition of Taino jades in eastern Cuba eventually spurred the recognition of the jadeites of Sierra del Convento (García-Casco et al. 2009, Cárdenas-Párraga et al. 2010), and in a reverse manner, the Río San Juan complex jadeites led to the sourcing of many Dominican Republic jades (Knippenberg et al. 2012; Schertl et al. 2012, 2014). One of the most recent putative discoveries is an unusual jadeite from the Torare River area of Papua, Indonesia, that was tracked from a jade gouge discovery on Emirau Island in the Bismarck Archipelago, Papua New Guinea, via rock specimens preserved at Utrecht University by C.E.A. Wichmann in 1893 (Harlow et al. 2012a,b). There are many jadeite jade objects from Europe, some of which have been tracked to the Monviso metaophiolite complex, western Italian Alps, Italy (e.g., Compagnoni & Rolfo 2003); however, other potential sources, such as the Queyras region of the French Alps and the Voltri Massif, western Alps, Italy, continue to be examined for potential (see Harlow et al. 2014). The point is that jade artifacts can show the way toward geological sources yet to be discovered. Jadeite has been routinely missed in regional geological surveys, but because our forebears were cognizant of the potential utility of rocks for tools, we can take advantage of their discoveries in our search for jadeite.

Jadeite, *sensu stricto*, is a rock consisting predominantly of jadeitic pyroxene—that is, >90 vol% pyroxene with on average at least 80 mol% jadeite, a clinopyroxene with end-member composition $\text{NaAlSi}_2\text{O}_6$. Jadeitic pyroxene typically occurs in a solid solution that is mostly binary toward diopside ($\text{CaMgSi}_2\text{O}_6$), with lesser hedenbergite ($\text{CaFe}^{2+}\text{Si}_2\text{O}_6$) and aegirine ($\text{NaFe}^{3+}\text{Si}_2\text{O}_6$), except for rare occurrences where jadeite-aegirine compositions are found (e.g., Papua; Harlow et al. 2012a,b). Practical definitions may be based on the term jadeite modified by another mineral for porphyroblasts, such as garnet, or for interbanding with glaucophane, phengite, or pumpellyite. Then there is the useful Russian-origin term apojadeite (i.e., formed from jadeite), which defines partially retrogressed or altered rocks typically containing veins or intergranular accumulations of albite, analcime, nepheline, diopsidic-acmitic (aegirine-rich) pyroxene, tremolite, etc. In some places, apojadeite is found more commonly than jadeite, and true jadeite deposits usually contain apojadeite.

3. LITHOLOGICAL AND GEODYNAMIC SETTING

The common thread of all jadeite occurrences is their association with serpentinite-matrix mélanges bearing other rocks or blocks with high-pressure/low-temperature (HP/LT) mineral



Figure 1

(a) Jadeite jade incense burner; China (Myanmar jade); late nineteenth century; 18 cm high (AMNH-MinCol. 44032, courtesy of American Museum of Natural History and Van Pelt Photographers). (b) Olmec jadeite jade celt; Miahuatlán, Oaxaca, Mexico; ca. 1500–1400 BCE; 10.5 cm long (AMNH-AnthroCol. 30/11518, courtesy of the Division of Anthropology, American Museum of Natural History, staff photo). (c) Jadeite jade magatamas from the second tomb of Sawano; Nara Prefecture, Japan; ca. 250–400 CE; largest ~3 cm long (courtesy of the Museum, Archaeological Institute of Kashihara, Nara Prefecture). Panel c modified with permission from Harlow et al. (2014).

assemblages. By this we mean the context of serpentinite from a convergent or transpressional setting that reflects the exhumation of a former mantle wedge boundary above a subduction channel. Unfortunately, massive serpentinites of this affinity have routinely been described as portions of an ophiolite. We consider this practice problematic, as ophiolites, even when not preserved with the major segments of their marine or oceanic setting, are generally characterized tectonically by obduction—overthrusting onto an “oceanic” margin—as opposed to exhumation from *HP/LT* conditions produced in a subduction channel. This origin is routinely reflected in the lack of a higher-*T* serpentinite polytype (antigorite) in true ophiolites except at their bases and the lack of associated *HP/LT* lithologies. The confusion may be increased by a not-too-unusual association

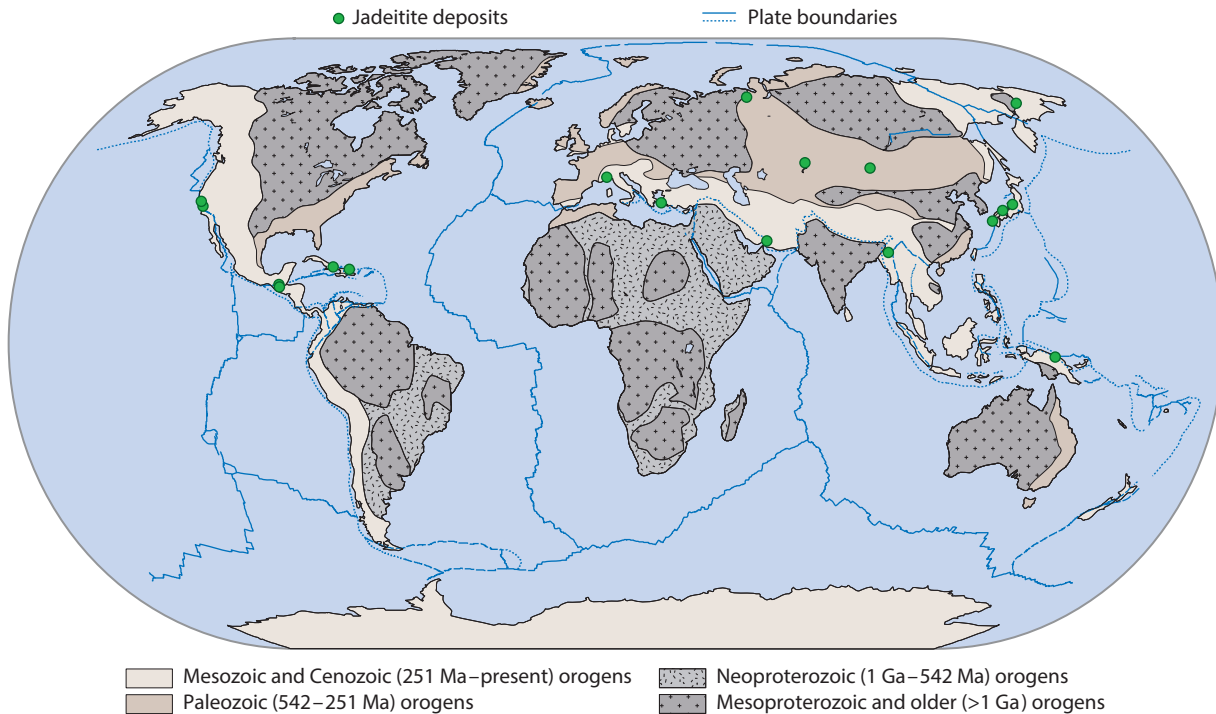


Figure 2

World map of jadeite occurrences and tectonic settings. Continental crust ages are modified after Tsujimori et al. (2006b). Figure modified with permission from Stern et al. (2013).

of paired *mélange*-ophiolite occurrences: for example, the Baja Verapaz and Sierra de Santa Cruz ultramafics (ophiolitic) north of the Northern Motagua *mélange* (NMM) in Guatemala (Harlow et al. 2011, Flores et al. 2013), the Moa-Barracoa ophiolite north of the Sierra del Convento *mélange* in eastern Cuba (García-Casco et al. 2009), and the Gaspar Hernandez serpentinite (ophiolitic) and the Arroyo Sabana and Jagua Clara *mélanges* in the Dominican Republic (Draper et al. 1991, Schertl et al. 2012). Distinguishing the serpentinite association is important for interpretation and exploration (Harlow & Flores 2011, Harlow et al. 2014).

P-type jadeite:

jadeite crystallized directly from a hydrous fluid as vein-fillings or overgrowths on other rocks

R-type jadeite:

a metasomatic replacement of another rock, such as a sedimentary rock (e.g., graywacke) or an igneous rock [e.g., trondhjemite or tonalite (mostly sodic feldspar + quartz)]

The occurrence of jadeite has been extensively reviewed (e.g., Harlow & Sorensen 2005; Harlow et al. 2007, 2014). More than 40 years after Coleman’s (1971) recognition of 6 “pure jadeite pod” localities, 19 jadeite localities have been reported in four Phanerozoic orogenic belts (Caribbean; circum-Pacific; Alps/Himalayas; Uralides and Central Asia/Altaids), excluding xenoliths in kimberlitic pipes (**Figure 2, Table 2**). Except for the xenoliths, these lie within serpentinite-matrix *mélanges*, with fragments of oceanic crust and *HP/LT* metamorphic rocks, along major transform or thrust faults cutting the paleo-forearc or accretionary wedge. Considering these worldwide occurrences, it is clear that serpentinite exhumation and *mélange* formation are important for the preservation of jadeite. These particular exhumation processes may also explain the rareness of jadeite occurrences.

On the basis of possible jadeite formation models, Yui et al. (2010) used the terms vein precipitation and metasomatic replacement for different jadeite origins; Tsujimori & Harlow (2012) then classified the two types as P-type and R-type, respectively. Precipitated jadeite does not contain evidence of a protolith and thus shows no evidence of isochemical transformation or

Table 2 Summary of jadeitites (types and ages) and associated mafic HP/LT metamorphic rocks

Locality	Type	Protolith age	Jadeite formation	Recrystallization or cooling	Associated mafic HP/LT rocks	Metamorphic age
Caribbean						
Northern Motagua mélange, Guatemala ^a	P _S	NA	Zrn: 98–95 Ma	Ph: 77–65 Ma	Ep-Gln eclogite, Grt amphibolite	Sm-Nd: 159–126 Ma (eclogite), Zrn: 76 Ma (eclogite in Chuactul ^b)
Southern Motagua mélange, Guatemala ^b	P _S , R?	NA	Zrn: 154 Ma	Ph: 125–113 Ma	Lws eclogite, Lws blueschist	Sm-Nd: 144–132 Ma (eclogite)
Sierra del Convento, Cuba ^c	P _S	NA	Zrn: 108–107 Ma	NA	Ep-Grt amphibolite, trondhjemitic Ep gneiss, blueschist	Zrn: 113 Ma (amphibolite)
Río San Juan complex, Dominican Republic ^d	P _B	Zrn: 139 Ma	Zrn: 115 Ma	Zrn: 93 Ma	Eclogite	Lr-Hf: 104 Ma (eclogite)
	P _B , R	Zrn: 113 Ma	Zrn: 117 Ma (core), 77.6 Ma (rim)	NA	Lws blueschist, Grt-Omp blueschist	Rb-Sr: 80, 62 Ma (blueschist)
Circum-Pacific						
Itoigawa-Omi, southwest Japan ^e	P _S , R	NA	Zrn: 520 Ma	Ph: 340–320 Ma	Ep-Gln eclogite, Ep blueschist, Ep-Grt amphibolite, metagabbro	Ph: 340–320 Ma
Oya-Wakasa, southwest Japan	P _S	NA	Early Paleozoic	NA	Lws-Pmp blueschist, Ep blueschist, amphibolite/metagabbro	Ph: 280 Ma (schist), Hbl: 470–440 Ma (Ep amphibolite, metagabbro)
Osayama, southwest Japan ^f	P _S , R	Zrn: 523–488 Ma	Zrn: 521–451 Ma	NA	Lws blueschist, Ep blueschist, Ep-Gln eclogite	Ph: 320 Ma
Nishisonogi, Kyushu, Japan ^g	R	Zrn: 142–131 Ma	Zrn: 82 Ma	NA	Ep blueschist	Ph: 90–75 Ma
Torare River, Papua, Indonesia	P	NA	Cretaceous–Paleogene?	NA	Amphibolite, blueschist?	NA
Ust-Belaya, Chukotka, Russia	P _S	Early Paleozoic	NA	NA	Grt amphibolite, blueschist	NA
New Idria, Franciscan complex, California	P _S	NA	Cretaceous?	NA	Lws blueschist, Ep eclogite, Grt-Cpx amphibolite	Hbl: 110 Ma (Grt amphibolite)
Ward Creek, Franciscan Complex, California	P _B	NA	Cretaceous?	NA	Lws blueschist, Pmp-Ep blueschist, Lws-Ep-Gln eclogite	Ph: 120 Ma (blueschist)

(Continued)

Table 2 (Continued)

Locality	Type	Protolith age	Jadeite formation	Recrystallization or cooling	Associated mafic HP/LT rocks	Metamorphic age
Alps/Himalayas						
Syros and Tinos, Cyclades, Greece ^h	P _S , R _S	Zrn: 80 Ma (in debate)	Zrn: 80 Ma (in debate)	NA	Ep-Gln eclogite	Zrn: 52 Ma, Ph: 52–43 Ma
Monviso, Western Alps	R _S	Zrn: 163 Ma	Eocene?	NA	Lws eclogite	Zrn: 163 Ma (relic), 45 Ma (metamorphic)
Sorkhan, Iran	P	NA	Cretaceous?	NA	Lws blueschist	Ph: 90–80 Ma
Jade Mine Tract, Myanmar ⁱ	P _S , R _S	Zrn: 163 Ma	Zrn: 158, 147, 122, 77 Ma	NA	Ep blueschist	Ph: 80 Ma (eclogite), 30 Ma (blueschist)
Uralsides						
Voikar-Syninsky, Polar Urals, Russia ^j	P _S	Early Paleozoic?	Zrn: 404 Ma	Zrn: 378, 368 Ma	Ep amphibolite (metagabbro), blueschist/eclogite	Zrn: 500 Ma (amphibolite), 360–355 Ma (eclogite)
Central Asia/Altaiids						
Borus Range, West Sayan, Russia	P _S , R _S	NA	Early Paleozoic?	NA	Eclogite	Zrn: 540–520 Ma
Kenterlau-Itmurunda-Arkharu, East Kazakhstan	P _S	NA	Zrn: 450 Ma	NA	Grt amphibolite, blueschist	Zrn: 450 Ma

Abbreviations: Hbl, hornblende K-Ar age; HP/LT, high-pressure/low-temperature; NA, not available; Ph, phengite K-Ar (or ⁴⁰Ar/³⁹Ar) age; Sm-Nd, Sm-Nd mineral isochron age; Zrn, zircon U-Pb age. See **Table 1** for mineral name abbreviations.

References for dating: ^aYui et al. (2010, 2012), Flores et al. (2013); ^bFu et al. (2010), Flores et al. (2013); ^cGarcía-Casco et al. (2009); ^dScherl et al. (2012), Hertwig et al. (2013); ^eKunugiza & Goto (2010); ^fTsujimori et al. (2005); ^gMori et al. (2011); ^hFu et al. (2010, 2012); ⁱShi et al. (2008), Qiu et al. (2009), Yui et al. (2012), Qi et al. (2014); ^jShatsky et al. (2000), Glodny et al. (2003, 2004), Meng et al. (2011). ^kDate from eclogite in the adjacent Chuacús gneisses (Martens et al. 2012). All other references are given in Tsujimori & Harlow (2012).

pseudomorphic replacement of any precursor rocks. The pervasive evidence for crystallization from a fluid includes jadeite grains that host abundant fluid inclusions (dominated by two-phase hydrous fluid, often in the cores of crystals); small preserved areas or veins of cavity filling, typically with oscillatory zoned jadeite prisms; and, in many cases, combinations of these features in brittly deformed/healed microtextures suggestive that the jadeitite ultimately formed in open veins but suffered severe deformation. These features have been revealed in colorful detail with cathodoluminescence microscopy, because low-Fe jadeite displays an array of colors documenting often subtle changes in composition (**Figure 3**). Most jadeitites belong to this P-type, and they are considered to have precipitated directly from a Na-Al-Si-rich aqueous fluid in some cavity, crack, or fracture in serpentinized peridotite or a *HP/LT* metamorphic rock. In contrast, replacive jadeitite partially preserves textural, mineralogical, or geochemical evidence of a preexisting protolith, such as plagiogranite or metagraywacke-like rock. Harlow et al. (2014) expanded this classification with a differentiation based on where the jadeitite was hosted (i.e., where the precipitate formed): P_S-type jadeitite is hosted in ultramafic (serpentinite) rock and P_B-type jadeitite in mafic (blueschist) rock. This distinction has potential importance for the source of the crystallizing fluid and its solute load (see below).

3.1. Where Jadeitites Form

There are few occurrences where jadeitite appears to remain in its formation setting, or nearly so, as the preponderance of jadeitite associations occur as blocks in serpentinite mélanges or erosional accumulations in drainages. The classic occurrence of a supposed dike hosted in ultramafic at Tawmaw, Myanmar (**Figure 4**), was a major reason for inferring an igneous origin as an albite granite subsequently modified by desilicification (Bleek 1908, Chhibber 1934). Two other interesting aspects of this occurrence are (*a*) the appearance of jadeitite at the center or core of the layer and albite toward the margin and (*b*) the asymmetry of the boundaries with the host ultramafic, with an amphibole-dominant rock (mostly sodic amphiboles) at the base and a chlorite-rich boundary layer on the hanging wall (essentially a blackwall reaction boundary). A similar association of jadeitite and albite or apojadeitite has been described in the Levoketchpel deposit, Polar Urals (Fishman 2006; see also Dobretsov 1984), but in the veins of the Pusyerka deposit of the Syum-Keu complex, also in the Polar Urals, no albite is found and the boundary between jadeitite and ultramafic is a phlogopite-anthophyllite lithology (Fishman 2006, Meng et al. 2011). Another contact has been reported in the Sierra de Las Minas, Guatemala, in which jadeitite is bounded by albite adjacent to a meta-ultramafic (chlorite-actinolite blackwall) and then a massive serpentinite (Sorensen et al. 2010). In all of these cases there is a mixture of primary jadeitite vein-like bodies, with or without an albite or apojadeitite outer boundary layer, separated from the host ultramafic by an amphibole rock or a chlorite-actinolite blackwall.

Jadeitite in contact with metabasite has been found in several places. In the Borus Mountains, West Sayan, Dobretsov (1984) interpreted the jadeitite as a metasomatic replacement: Rims of eclogite blocks are replaced by omphacite and then surrounded by small bodies of jadeitite, like a necklace, in the sheared serpentinite matrix. However, no relics of eclogite were described in the jadeitite, so replacement is not absolutely clear. A similar occurrence was described for jadeitite from Syros, Cyclades, Greece, in which jadeitite appears to fill fractures in eclogite blocks, an interpretation supported by the lack of relict garnet (Bröcker & Keasling 2006). An igneous protolith to the jadeitite was ruled out by the presence of *HP* inclusions in zircon in the jadeitite. Jadeitite has been found as concordant layers in blueschist in the Río San Juan complex mélange, Dominican Republic, and as jadeite-quartzite or jadeite-lawsonite-quartzite mostly in discordant tension gashes (Schertl et al. 2012); the jadeitites (*sensu stricto*) may be R- or P-type,

Protolith: the original type of rock, such as basalt, prior to metamorphism (e.g., to an eclogite or blueschist) or metasomatism

Blueschist: an *HP/LT* metamorphic rock formed from basalt by hydration and dominated by the blue amphibole glaucophane; also the facies, or *P-T* region, for blueschists

Omphacite: a rock composed principally of clinopyroxene of omphacite composition, nominally $(\text{CaNa})[(\text{Mg,Fe})\text{Al}](\text{Si}_2\text{O}_6)_2$ and a variety of jade

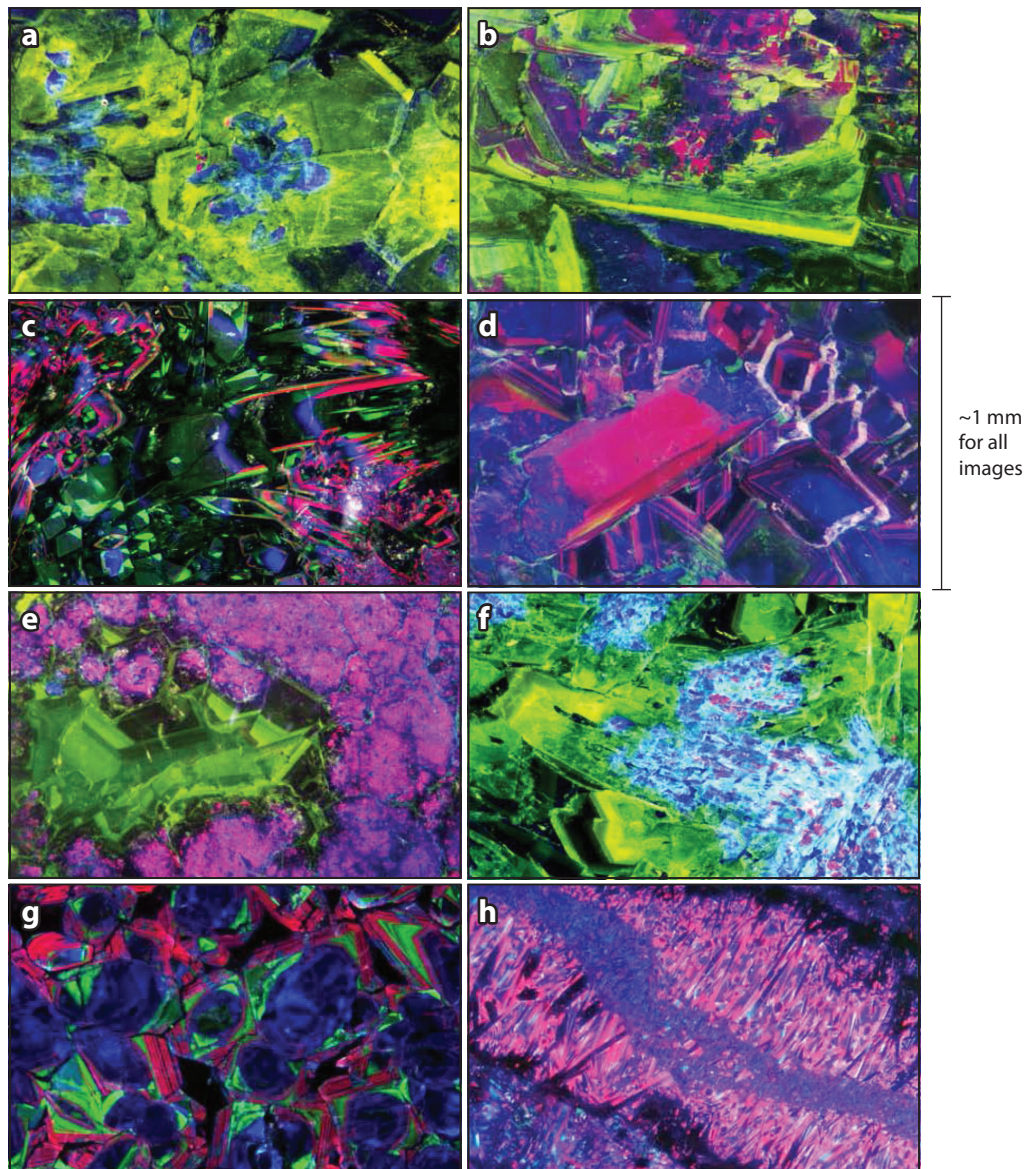


Figure 3

Cathodoluminescence images of jadeitites. (a) American Museum of Natural History (AMNH) Specimen 104278; Ketchpel River, Polar Urals, Russia. (b) National Museum of Natural History (NMNH) Specimen 112701; Myanmar. (c) AMNH Field Number 01GSn6-13 (Virginia Sisson); Guatemala. (d) NMNH Specimen 94303; Myanmar. (e) AMNH Field Number MVJ84-9D (George Harlow); Guatemala. (f) NMNH Specimen 105860; Japan. (g) AMNH Field Number MVE02-3-1 (Sorena Sorensen); Guatemala. (b) NMNH Specimen 113778-1; California. All specimens were irradiated at 20 kV and 0.5 mA. The images in panels *c* and *g* were collected by an Olympus CCD camera using MagnaFire 2.0 software; the others are scanned emulsion images. All panels show the growth of extremely idioblastic grains, oscillatory zoning, and apparent infilling of fluid-filled spaces; panels *a*, *b*, and *f* also show apparent resorption and overgrowth features. Panel *b* additionally shows grain-size reduction and the entrapment of brecciated vein-forming grain fragments along a sheared surface that cuts an earlier-formed vein. Figure modified with permission from Harlow et al. (2014).

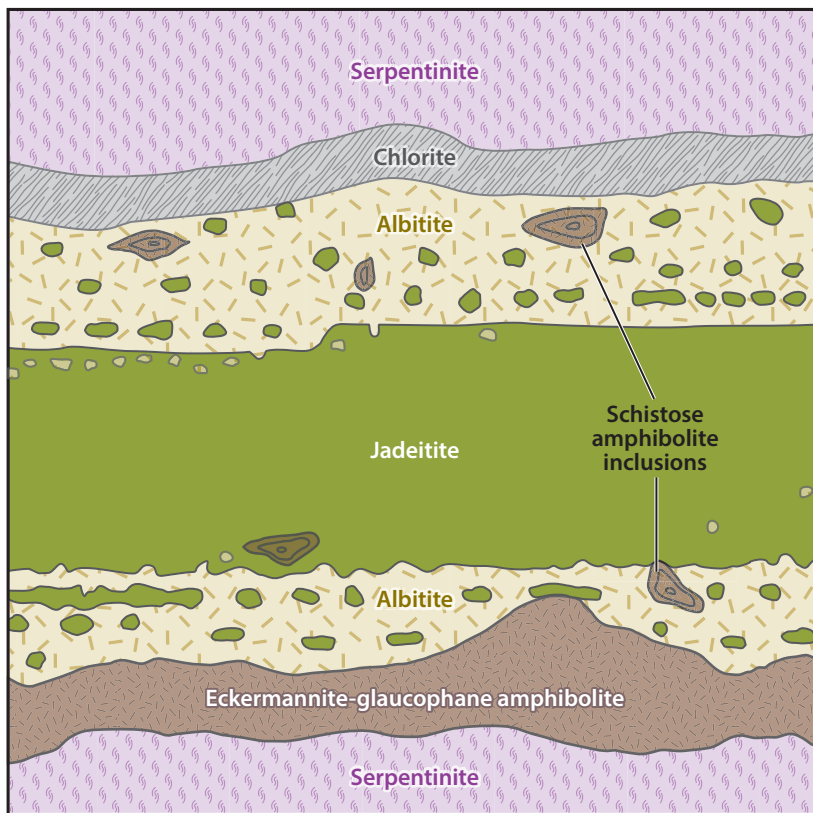


Figure 4

Diagram of contact relationships of the jadeitite dike at Tawmaw, Myanmar, after figure 3 from Bleek (1908). No dimensions were given in that source, but other sources (e.g., Chhibber 1934, Hughes et al. 2000) indicate that the width can vary between 1.5 and >50 m and the length can exceed 1 km. The described pinching and swelling of these dikes suggest considerable tectonic deformation.

as work continues on these samples. However, the clear distinction here and at a couple of other occurrences (see Harlow et al. 2014) is that fluid-crystallized jadeite occurs without the immediate proximity of an ultramafic host. This feature led to their classification as either R_B - or P_B -type jadeite.

3.2. Estimating P - T Conditions of Jadeitite Crystallization

Estimating P - T conditions for a rock that is nearly monomineralic relies on small variations in composition, associated minerals that are minor and not developed in every jadeitite body or locality, and techniques other than phase equilibria (e.g., coexisting rocks). Tsujimori & Harlow (2012) have reviewed the available information in detail, so only a general synopsis is provided here. Harlow (1994) used the reactions $Anl = Jd + H_2O$, $Ab = Jd + Qz$, and $4Lws + 2Jd = Ab + Pg + 2Czo + 6H_2O$ (with lowered activities of some components) to pose a possible limit on the upper P - T stability of quartz-free jadeitite (and when albite may be secondary) of ~ 1.4 GPa and $\sim 450^\circ\text{C}$ (Figure 5a). The presence of jadeite and the absence of quartz yield a lower limit for P estimates, fundamentally limited by either the reaction $Anl = Jd + H_2O$ in the presence of

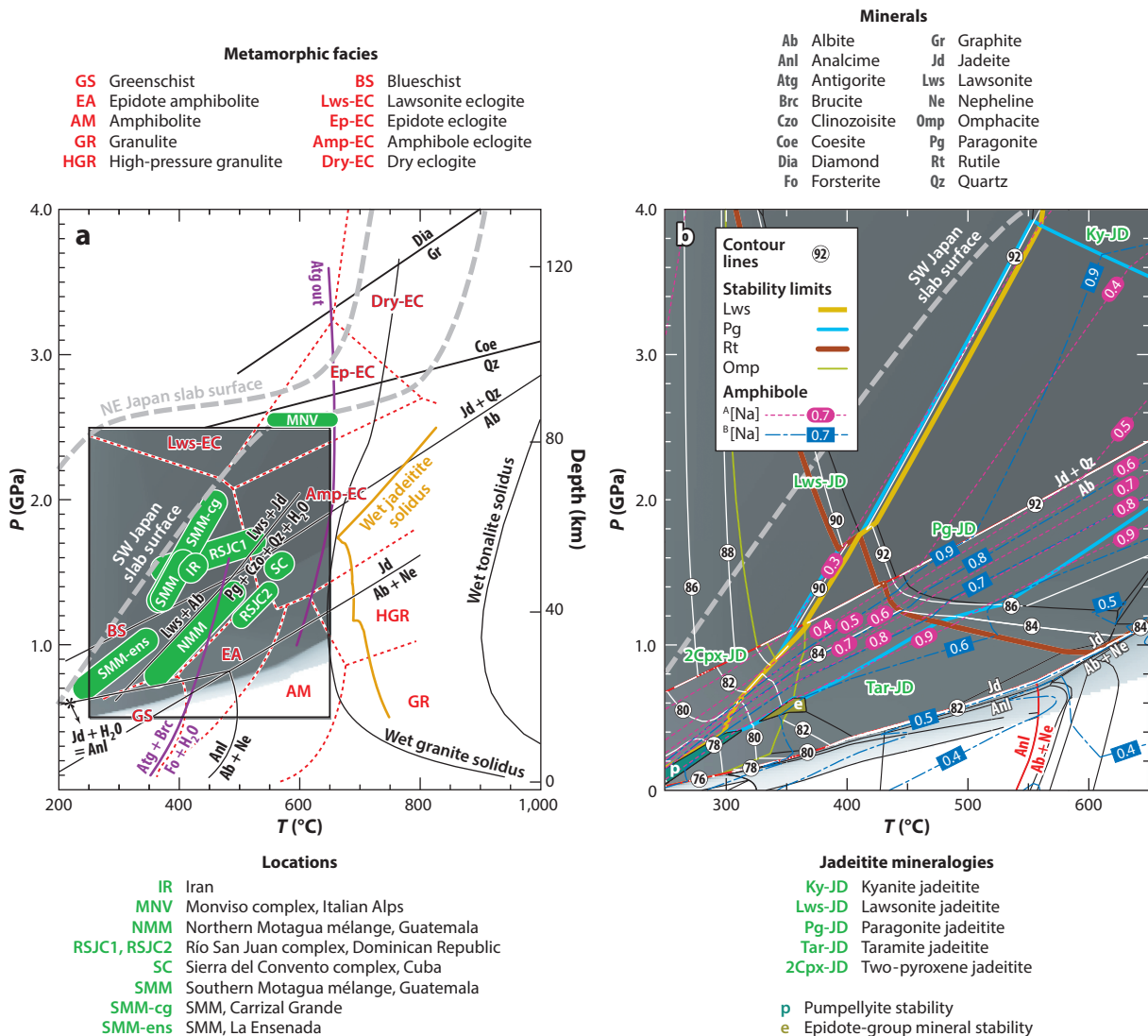


Figure 5

(a) Pressure-temperature (P - T) diagram showing approximate P - T conditions of selected jadeitites from Guatemala, Cuba, Iran, the Dominican Republic, and the Italian Alps (modified with permission after Tsujimori & Harlow 2012, Harlow et al. 2014). Also shown are reaction curves limiting jadeitite-bearing mineral equilibria, the Atg-out reaction, and Pg + Czo assemblage, as well as the modelled wet jadeitite solidus (this review) and P - T paths (model D80 of Syracuse et al. 2010) for slab surfaces in both warm (Nankai, southwest Japan) and cool (Tohoku, northeast Japan) subduction zones. The metamorphic facies boundaries are after Maruyama et al. (1996) and Liou et al. (2004); a boxed P - T space (250–650°C and 0.5–2.5 GPa) delineates the P - T pseudosection shown in panel *b*. (b) P - T pseudosection calculated for the average SMM jadeitite composition (with the atomic ratios Si:Ti:Al:Fe:Mg:Ca:Na:K:O = 51.06:0.06:23.56:0.54:1.05:1.31:22.13:0.29:151.69) in the NCFMASHT (NaO-CaO-FeO-MgO-Al₂O₃-SiO₂-H₂O-TiO₂) system with excess H₂O; 0.1 mol C to stabilize CH₄ was added to buffer oxygen fugacity. The color gradation level represents the modal volume of jadeitic clinopyroxene; thin white lines with white-circled numbers are contour lines of this modal volume percentage. Contours of amphibole composition (Na fraction in the A- and B-sites) are also shown as magenta and dark blue dotted lines.

aqueous fluid or the reaction $Jd = Ne + Ab$ when relatively dry. The resulting limits are ~ 0.6 GPa at 200°C or ~ 0.7 GPa at 400°C for the former reaction and ~ 0.15 GPa at 200°C or ~ 0.65 GPa at 400°C for the latter reaction. As fluid inclusions and healed cavities and veins are common in jadeitites, an aqueous fluid is more than likely during formation. Fluid inclusion data reported by Johnson & Harlow (1999) for Guatemalan jadeitite (quartz-free, north of the Motagua fault zone) yield a lower T limit of $\sim 272^\circ\text{C}$. These authors also calculated T based on the fractionation of ^{18}O between albite and muscovite, which yields $T = 327^\circ\text{C} \pm 50^\circ\text{C}$ for an albitite, and between jadeite and albite, which yields $T = 401^\circ\text{C} \pm 50^\circ\text{C}$; five ^{18}O temperatures for albite-muscovite pairs range from 283°C to 302°C (Johnson & Harlow 1999). Sorensen et al. (2006) measured $\delta^{18}\text{O}$ for a jadeite-albite pair from a Myanmar jadeitite, which yielded a best T estimate of 257°C and argued for LT formation. Shi et al. (2003) constrained crystallization of an amphibole-bearing Myanmar jadeitite in a manner similar to Harlow (1994) with the addition of NaMgAl -amphibole reactions and fluid inclusion data to estimate $T = 250^\circ\text{C}$ to 370°C at $P = 1$ to ~ 1.2 GPa. For Osayama, Japan, quartz-free jadeitite, homogenization T (T_h) for two-phase aqueous fluid inclusions led Shoji & Kobayashi (1988) to estimate a minimum jadeite crystallization $T = \sim 345^\circ\text{C}$. Tsujimori et al. (2005) used ThermoCalc software and the phase assemblage of $Jd + Rt + Grs$ to estimate $P > 1.2$ GPa at 200 – 300°C .

For jadeitites manifesting $Qz + Jd$, P must exceed that defined by the $Ab = Jd + Qz$ reaction. For jadeitite from Carrizal Grande, Guatemala, the combination of $Qz + Jd$ and Lws indicates higher P and lower T , consistent with the lawsonite-blueschist facies (SMM-cg in **Figure 5a**; Tsujimori et al. 2006a): $P > 1.2$ GPa and $T = 300$ – 450°C . Coexisting omphacite-jadeite in these jadeitites suggests low T relative to the crest of the solvus of Carpenter (1981) at $\sim 600^\circ\text{C}$ or of Green et al. (2007) at $\sim 700^\circ\text{C}$, with pairs estimated between $\sim 200^\circ\text{C}$ and $> 500^\circ\text{C}$ (Harlow et al. 2011). For jadeitite from Tone, Japan, Czo coexists with $Qz + Jd$, so Shigeno et al. (2005) interpreted crystallization at $T > 400^\circ\text{C}$ and $P \geq 1.3$ GPa. Jadeitite from Sierra del Convento represents a source yielding higher temperatures, $\sim 550^\circ\text{C}$, from coexisting omphacite-jadeite compositions, at P of 1.5 GPa interpreted from the *mélange* (García-Casco et al. 2009, Lázaro et al. 2009). The two different Río San Juan complex jadeitites yielded different conditions. Quartz-bearing jadeitites from blueschist were evaluated through the presence of lawsonite and glaucophane, Si content in phengite, and a reasonable P - T - t path as forming at 350°C to 550°C and 1.4 to 1.7 GPa (RSJC1 in **Figure 5a**), with the possibility of higher P . A similar evaluation for quartz-free jadeitites and the thermal structure of the subduction zone yielded 480°C to $\sim 580^\circ\text{C}$ and ~ 1 to ~ 1.3 GPa (RSJC2 in **Figure 5a**), roughly between the fields for the NMM and Sierra del Convento complex.

Another approach for determining P - T conditions is via the use of pseudosections, which are based on whole-rock compositions and calculated limiting phase assemblages. Oberhänsli et al. (2007) performed such an analysis on Iranian blue jadeitite (assemblage: $Jd + Lws + Ktp$) using the Theriak-Domino software (de Capitani & Petrakakis 2010) and obtained 400 – 450°C at 1.6–1.7 GPa. A P - T pseudosection (equilibrium phase diagram) calculated for natural jadeitite in the model system NCFMASHT ($\text{NaO-CaO-FeO-MgO-Al}_2\text{O}_3\text{-SiO}_2\text{-H}_2\text{O-TiO}_2$) is shown in **Figure 5b**. The average composition (59.13 wt% SiO_2 , 0.09 wt% TiO_2 , 23.14 wt% Al_2O_3 , 0.75 wt% FeO^* , 0.02 wt% MnO , 0.82 wt% MgO , 1.42 wt% CaO , 13.22 wt% Na_2O , 0.26 wt% K_2O , 0.01 wt% P_2O_5 , where FeO^* is the total amount of oxidized iron expressed as FeO) of 24 Southern Motagua *mélange* (SMM) jadeitites was used with excess H_2O ; MnO and P_2O_5 were neglected. Calculation was performed using the Theriak-Domino software (de Capitani & Petrakakis 2010) with the internally consistent thermodynamic data set of Holland & Powell (1998); solution models suggested by Green et al. (2007), Dale et al. (2005), and Coggon & Holland (2002) were used for clinopyroxene, amphibole, and white mica, respectively. Modal

Basalt: the most common form of lava on Earth, typically with 48 to 53 wt% SiO₂

volume of jadeite and amphibole compositions were also calculated. In the P - T pseudosection, the stability fields of lawsonite, paragonite, Ca-Na amphibole (taramitic), two coexisting pyroxenes, and kyanite predict five mineralogical types of jadeitite, namely lawsonite jadeitite, paragonite jadeitite, taramite jadeitite, two-pyroxene jadeitite, and kyanite jadeitite (**Figure 5b**). Moreover, the transformation of titanite-bearing to rutile-bearing mineral assemblages may further separate rutile-bearing jadeitite from rutile-free jadeitite. The modal volume of jadeitic pyroxenes reaches 92 vol% in the paragonite jadeitite field. Although the petrogenetic nature of jadeitite may cast doubt on the reliability of thermodynamic modelling—especially modelling with a fixed bulk-rock composition, silica activity, etc.—the chemographic relations in P - T space are still helpful for understanding the natural parageneses of jadeitites. For example, previous P - T estimates for lawsonite-bearing jadeitites with a trace amount of quartz and/or glaucophane from the SMM and taramite-bearing, lawsonite-free jadeitites from the NMM fit P - T ranges of the inferred mineralogical types of jadeitite. It is also important that the pumpellyite stability field lying at the lower- T side of the epidote stability field is consistent with natural observations in Guatemala, whereas the stability field of epidote-group minerals is highly controlled by the oxidation states of iron and manganese—i.e., oxygen fugacity. Our P - T pseudosection predicts kyanite-bearing jadeitite at $P > 2.4$ GPa and $\sim 600^\circ\text{C}$ that has not yet been reported. In the Monviso metaophiolite, R-type jadeitite with a plagiogranite protolith was estimated to have formed in the kyanite jadeitite field (**Figure 5a,b**). However, the absence of kyanite in Monviso jadeitite is likely due to a less aluminous bulk-rock composition.

The calculated wet solidus of an SMM jadeitite composition is shown in **Figure 5a**. Solution models that Nagel et al. (2012) used to obtain the wet solidus of normal mid-ocean ridge basalt (N-MORB) and tholeiite (a subtype of basalt) were applied for our calculation. The modeling suggests that initial partial melting of jadeitite occurs at >670 – 700°C and 1.2–1.7 GPa (higher than the temperature of antigorite breakdown) and that the temperature along a steady-state subduction interface does not exceed the wet jadeitite solidus. Although the mantle wedge where P-type jadeitite forms is warmer than the underlying slab surface, jadeitite does not melt throughout the underflow of jadeitite-bearing mantle wedge slices and mélanges in steady-state subduction zones. In fact, xenoliths of “jadeitite” (eclogite containing up to 93 vol% jadeitic pyroxene) and metasomatic omphacite (Watson & Morton 1969, Schulze et al. 2014) that have no partial melting, together with coesite-bearing lawsonite eclogite and antigorite serpentinite, were transported from sinking of the Farallon plate by Oligocene kimberlitic plume upwelling. In the case of a non-steady-state scenario such as spreading-ridge subduction and hotter asthenospheric flow into the mantle wedge, however, preexisting jadeitite remaining at the base of the mantle wedges may melt due to warming of the geotherm.

3.3. How Jadeitite Forms

All of the contexts in which jadeitite is found are associated with rocks in the subduction channel or with the serpentinite formed by antigorite serpentinization of peridotite, presumably from the overlying mantle wedge (**Figure 6**). Several aspects of the latter—and most common—occurrence are important. For a hydrous fluid to form a vein in peridotite or serpentinite, brittle fracture is required (**Figure 7**). Many arguments are made that cold, brittle, decoupled noses of the mantle wedge in subduction zones are decoupled because they are brittle and are limited to depths shallower than the decoupling depth of 75 ± 15 km (Wada et al. 2008). However, evaluations of whether the ultramafics along the subduction channel boundary should deform by brittle deformation are mixed (see Hirth & Guillot 2013). The conditions reported for all jadeitite, with maximum $P < 2.5$ GPa and $T < 600^\circ\text{C}$ and more generally $P < 2.0$ GPa and $T < 500^\circ\text{C}$, are reasonable for

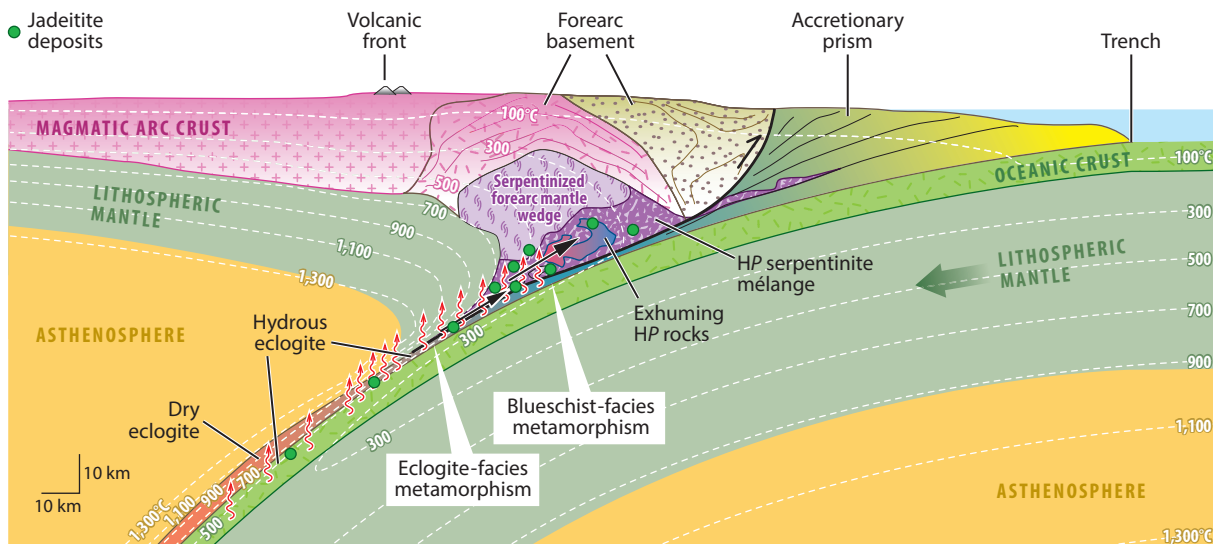


Figure 6

Cross section showing a Phanerozoic Pacific-type subduction zone where jadeite forms (modified after Stern et al. 2013, Tsujimori & Ernst 2014). Lithological variations and thermal structures are based on numerical modelling by Gerya (2011). Temperature contours (dashed white lines) are in degrees Celsius. Inferred occurrences of jadeite in the cross section are denoted by green circles. P-type jadeite forms in fractures in serpentinizing mantle wedge peridotite. Abbreviation: HP, high-pressure.

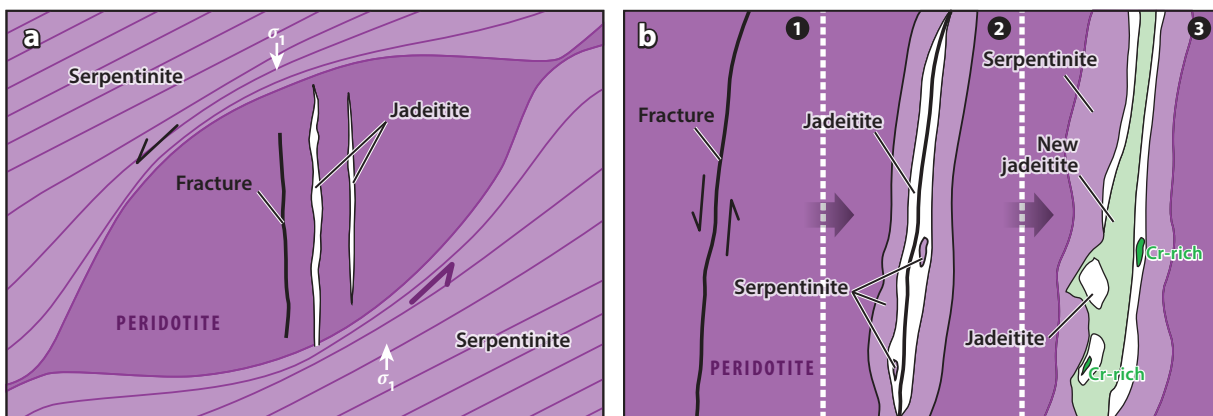


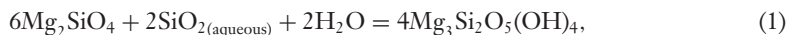
Figure 7

Diagram of a model for jadeite formation in veins in peridotite. (a) A boudinaged, less-serpentinized peridotite with hydrofractures where jadeite precipitation occurs (P-type jadeite). This model is based on figure 3 from Nicolas & Jackson (1982) (boudinaged pyroxenite layer with syntectonic gabbroic veins). σ_1 is the maximum principal stress direction. (b) Stepwise fluid infiltration along the fracture/fault to form multigeneration P-type jadeite (after Harlow & Sorensen 2005). As in **Figure 4**, the width of these veins and blocks can vary from about 1.5 to 50 m.

the P - T interpretations along the boundary of the mantle wedge nose and the subduction channel in representative systems (e.g., Peacock 2001, Deschamps et al. 2013). The presence of antigorite rather than lizardite in the associated serpentinites further constrains temperatures to be above $\sim 300^\circ\text{C}$ (Evans 2004) unless talc is present, for which $T > \sim 200^\circ\text{C}$. Alternatively, hydrous fluid entering peridotite without serpentinization requires only $T = \sim 430^\circ\text{C}$ at 0.7 GPa, where jadeite is stable relative to analcime (**Figure 5a**). Our own observations of antigorite veins in antigorite blocks from jadeitite-bearing mélanges and the macroscopic dikes noted above argue that there is brittle deformation and vein formation in the mantle wedge above the subduction channel. In support, Nicolas & Jackson (1982) have described gabbroic dikes/veins cutting a boudinaged pyroxenite layer within mylonitized peridotite from New Caledonia; the gabbroic dikes were injected into the extension plane related to the deformation. In the mantle wedge and the subduction channel, through a similar mechanism, it would be highly possible that rigid, less-serpentinized peridotite portions are boudinaged within plastic, highly serpentinized peridotite or serpentinite by their ductile deformation (**Figure 7a**). Considering the extensive heterogeneous distribution of serpentinization in most jadeitite-bearing mélanges as well as on-land analogs of forearc mantle sections, the heterogeneity of serpentinization and stress/strain in ultramafic rocks above the subducting slab would be an essential trigger for the formation of fractures where P-type jadeitites can form.

Another factor in forming veins is the hydrofracturing that is needed to drive the vein fluid into the host rock and is clearly expected in the context of fluid along a fault boundary, such as along the subduction channel–mantle wedge boundary. Such events, as recorded by jadeitites worldwide, appear to be highly repetitive within jadeitites. Abundant growth bands, seen both in cathodoluminescence and in backscattered electron imaging or X-ray mapping with the scanning electron microscope, document fractures that have been infilled by later jadeite (see **Figure 3**). Brittle deformation, probably in the form of hydrofracture, apparently allows fluid access to jadeite masses. Some jadeitites show evidence for grain-boundary fluid percolation, seen in a new generation of jadeite that decorates an aggregate of grains with different compositions. Other specimens contain shear zones that evidently comminuted grains by orders of magnitude. In a few rocks, jadeite grains show partially resorbed cores of one composition, surrounded by growth-zoned, idioblastic jadeite. Jadeitites obviously testify to a dynamic formation environment within host serpentinite. Moreover, they suggest that the jadeite veins appear to focus fracturing within serpentinite, thus permitting the growth bands to be internal to the deformed solid jadeite, in many cases with cavity fillings along apparent fractures, rather than external overgrowths on veins.

Jadeitite formation by fluid entering fractures in the serpentinizing mantle wedge has several distinct consequences. If the ultramafic is incompletely serpentinized, it will act like a sponge for the H_2O and silica from the fluid during continued serpentinite formation. This results from the following idealized reaction (simplified and ignoring the difference between lizardite and antigorite stoichiometry):



which avoids formation of brucite (not reported from serpentinites associated with jadeite). This sponge effect for H_2O should assist in crystallization in veins by inducing supersaturation of the remaining fluid. Additionally, many ultramafic-hosted jadeitites (e.g., Myanmar, the NMM) are quartz free, which may well be the result of the reduced silica activity (Harlow 1994, Harlow et al. 2014). Another indication that this active serpentinization is involved in jadeite vein crystallization is the presence of late-stage Ca enrichment in and around jadeite bodies, particularly the late omphacitites. Clinopyroxene is one of the last phases to break down in peridotite during serpentinization, so its release into the hydrous fluid will be an indication of serpentinization

reaction progress. Similarly, the breakdown of chromite in ultramafics is a late-stage process, which is recorded by Cr-richer (emerald-green) jadeite via late-stage veining and tectonic admixing. Finally, this evolution is consistent with the observation that nearby serpentinite hosts of jadeitites contain few, if any, relict peridotite minerals (e.g., Coleman 1961, Harlow 1994).

Thus, a model for jadeitite crystallization in fractures in mantle wedge peridotite envisions stepwise fluid infiltration along the fracture or fault, with progressive addition of jadeite to jadeitite (**Figure 7b**). As a conduit for fluid into peridotite, serpentinization should zone outward from the large fracture by a mixture of grain boundary-driven and expansion-driven fracture, probably similarly to the case for peridotite carbonation as discussed by Kelemen et al. (2011). However, major fracturing apparently focuses along the vein and through the brittle jadeitite. Subduction-driven deformation leads to pinching and swelling, as with tension gashes, and rotation that produces blocks as well as veins. How this process relates to the formation of an active subduction channel mélange is unclear, but data on the timing in relation to exhumation are now being assessed, as discussed below.

The interpretation of the formation of jadeitite as a metasomatic replacement of a protolith has evolved over the years. The igneous albite granite dike interpretation for the Tawmaw, Myanmar, deposit invoked gain of Na_2O and loss of SiO_2 without addressing the issue of pressure (e.g., Bleeck 1908, Chhibber 1934). Dobretsov & Ponomareva (1965) argued for a similar process with leucogabbros and granitoids included in the serpentinite from the Polar Urals and Itmurundy, Kazakhstan. A lack of any unmetasomatized bodies for these and other cases led to an interpretation of wholesale metasomatism of blocks in mélanges for the above locations and for Guatemala (da Silva 1967, 1970; McBirney et al. 1967; Bosc 1971). Generally, the lack of pseudomorphism, the relics of protolith minerals, and the rhythmically zoned jadeite grains in the jadeitites from these locales have eaten away at the metasomatism arguments.

More recent descriptions of jadeitites from the western Italian Alps and the Nishisonogi complex, Japan, have better established metasomatic (R-type) jadeitite. Compagnoni & Rolfo (2003) and Compagnoni et al. (2012) have identified relics of igneous pyroxene in the cores of jadeite grains in a jadeitite block from Punta Rasciassa, Monviso metaophiolite, in support of the metasomatic replacement of metagabbro. In addition, stringers of rutile running through the sample suggest boudinage of a mafic protolith. Shigeno et al. (2012) observed quartz inclusions in jadeite grains in jadeitite from Tone and Mie in the Nishisonogi complex, for which micromodal analysis is consistent with a local replacement of albite. Nonetheless, both sets of authors observe jadeite overgrowths on these cores and in these jadeitites, indicating that they have a P-type crystallization component.

As the context of R-type jadeitite requires a mafic to felsic protolith, either rocks from the subduction channel or igneous intrusions into ultramafic must be involved. For the Tone jadeitite, an acid igneous rock—probably a plagiogranite (trondhjemite-tonalite)—was believed to be the protolith, on the basis of the inclusions in and the trace element patterns of relict igneous zircons, which also recorded the igneous age (see below; Mori et al. 2011). In a somewhat different context, García-Casco et al. (2009) interpreted the jadeitite of the Sierra del Convento mélange as being primary jadeitite but resulting from the complete metasomatic replacement or dissolution and precipitation of components from peraluminous tonalitic-trondhjemitic rocks in the upper plate, which in turn formed from partial flux melting of mafic amphibolites from the subduction channel that had been accreted to the sole of the upper plate. This might be the context of the Tone felsic protolith as well. Alternatively, tonalite-trondhjemite-diorite suites are the lithologies grouped as plagiogranites in oceanic settings formed near spreading centers and preserved both in classic obducted (or accreted) ophiolites (see Dilek & Furnes 2014) and in suprasubduction settings from melting of young amphibolites of a subducted spreading center (hot subduction and

shallow melting; Shervais 2001, 2008); however, how the latter might get into a *HP/LT* environment is an interesting question. In their study of jadeitite and jadeite-quartz rock from the Monviso metaophiolite, which is composed of subducted crust in a near-slow-spreading-ridge setting, Compagnoni et al. (2012) demonstrated a close concordance between the whole-rock composition signatures of metaplagiogranite, jadeitite, and jadeite-quartz rock, as well as a similarity in the zircons in the three rock types. They concluded that the jadeitite was derived from a plagiogranite protolith.

Finally, there are those jadeitites included in blueschists (P_B - or R_B -type) and other metabasites, such as in the Río San Juan complex mélange. These rocks, which can be either true jadeitites containing little other than jadeite or jadeite-bearing rocks containing considerable quartz, lawsonite, etc., have recently been recognized as a distinct type of jadeitite. Although they are part of serpentinite-bearing mélanges, they are probably derived from fluids permeating the metabasites; it is not yet clear whether serpentinites play a significant role in their formation. There appear to be many similar occurrences of small jadeite veins in metabasites [e.g., Escambray massif, Cuba (Maresch et al. 2012); Ward Creek, Franciscan complex, California (Tsujimori & Harlow 2012)], where similar processes are at work but the veins do not become magnified by some repetitive process to yield blocks that would be considered separate rocks (or jade).

4. FLUIDS, SOLUTES, SOLUBILITIES, AND SOURCES

Given the strong evidence for crystallization of jadeitites from—or even metasomatic modification of a protolith by—a fluid, determining that fluid’s characteristics, source, and solute load is critically important.

4.1. Fluid Compositions

Various lines of evidence reveal the composition of the fluid. Fluid inclusion salinities and O/H isotopic systematics in jadeitites from the NMM have been interpreted to indicate the predominance of a seawater-like fluid that is entrained during subduction rather than being the product of dehydration of deep metamorphic minerals (Johnson & Harlow 1999). Sisson et al. (2006) have examined fluid inclusions further, finding two-phase aqueous inclusions with salinity ranges from 2 to 8 wt% NaCl equivalent and T_h from 170°C to 300°C. In the SMM, inclusions in jadeite are predominantly two-phase aqueous with salinity ranges from 0 to 3 wt% NaCl equivalent and T_h from 115°C to 200°C, but there are some one-phase inclusions and rare CH_4 - H_2O inclusions. None of the two-phase inclusions are sufficiently dense to have been preserved from the growth conditions, implying either erroneous estimates of growth conditions or some stretching since entrapment; the authors favor the latter. Moreover, the range in salinities suggests different fluids in the NMM versus the SMM: saltier and less salty than seawater, respectively. Fluid inclusions in Hpakan, Myanmar, jadeite also show H_2O -rich and CH_4 -rich fluid compositions, between 3.0 and 8.5 wt% NaCl equivalent and with T_h from 315°C to 378°C (Shi et al. 2005). The T_h values appear high, particularly in comparison with Guatemalan samples that otherwise have a similar interpreted P - T - X origin. Possibly, the Myanmar jadeite inclusions were all reset during exhumation. However, the authors did not present enough data about the sizes of fluid inclusions to determine whether this is the case. Isotopic measurements by Shi et al. (2005) yielded $\delta^{13}C$ (CH_4) from -30.1‰ to -25.5‰ and δD (H_2O) from -56.3‰ to -48.8‰ ; these findings were interpreted as indicating abiogenic methane produced by thermal maturation of subducted organic carbon and either a metamorphic fluid contribution to the D/H systematics or later diffusional exchange with the enclosing serpentinite. The authors also argued for immiscible liquids for the

two different kinds of inclusions but did not provide much evidence. This latter point contrasts with the observation of heavier H in the Guatemalan rocks; however, the measurements are on different phases in the rocks. By comparison, both primary and secondary fluid inclusions in eclogite and garnet amphibolite samples from the Franciscan complex and Catalina schist, California, and the Samaná Peninsula, Dominican Republic, preserve seawater-like salinities (Sorensen & Barton 1987, Giaramita & Sorensen 1994). Meng et al. (2011), in their research on jadeitite from Syum-Keu, have reported both H₂O-rich and CH₄-rich fluid inclusions, which they describe as one-phase but are clearly imaged as two-phase; no interpretation was made about these inclusions other than their consistency with prior research on jadeitite. For Osayama quartz-free jadeitite, T_h for two-phase aqueous fluid inclusions led Shoji & Kobayashi (1988) to estimate a minimum jadeite crystallization T of $\sim 345^\circ\text{C}$.

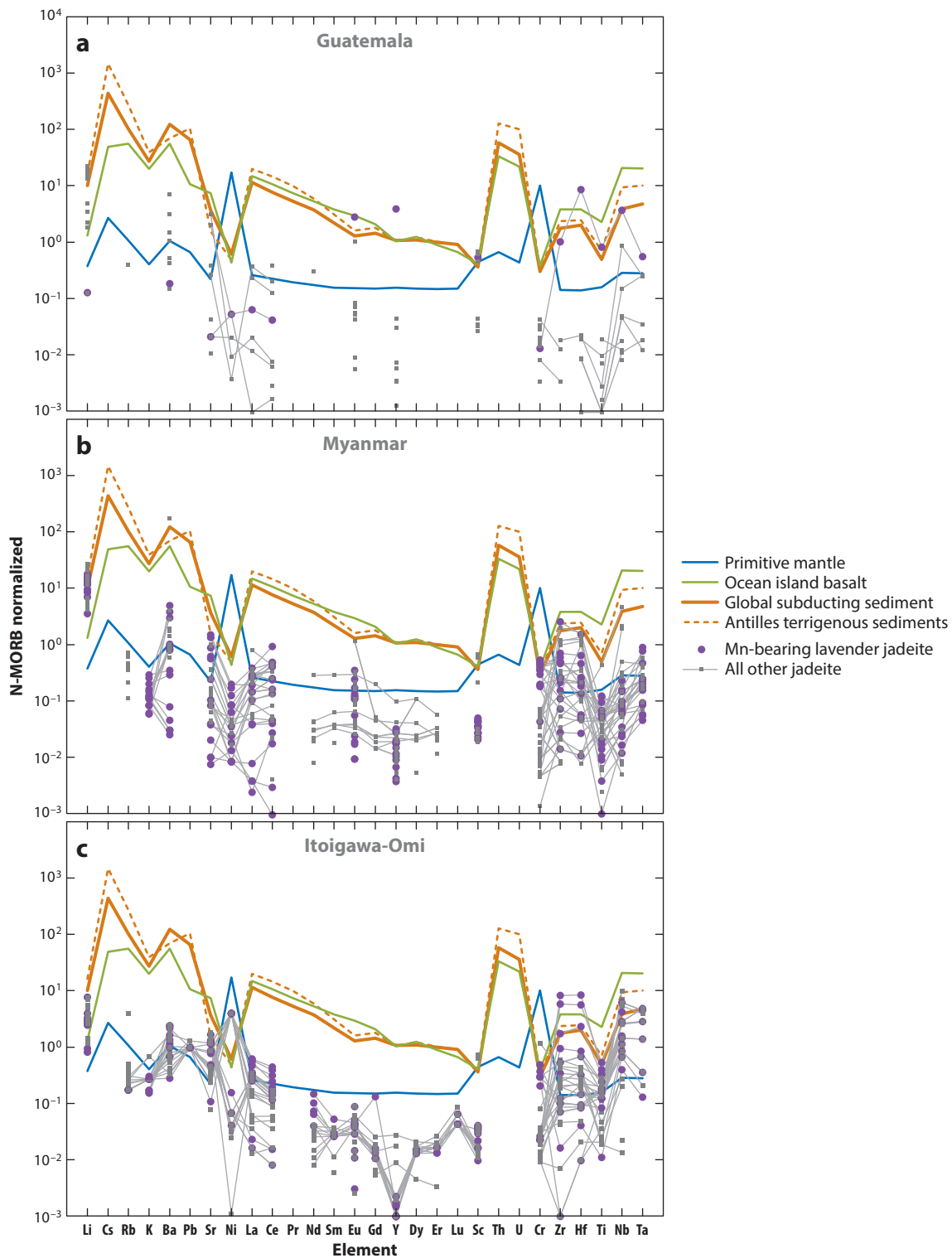
Beyond the above interpretations, we have observed hydrous and some gas fluid inclusions in the thin sections of jadeitites we have observed, which represent many of the 19 occurrences; however, we have not done detailed studies beyond those cited above.

4.2. Source of Solutes Inferred From Jadeitite Samples

For a P-type jadeitite, if the model is correct, the bulk composition must reflect the geochemical transport of species dissolved in the fluid from its source and pathways and deposited by crystallization in its host. So, what are the characteristics of jadeite in jadeitite as well as whole-rock compositions beyond the simple dominance of a jadeite-like composition?

In an electron and ion (secondary ion mass spectrometry) microprobe study guided by cathodoluminescence images of zoning in jadeite grains in jadeitite from Myanmar, Guatemala, Japan, Kazakhstan, and California, Sorensen et al. (2006) reported consistent trends of increasing Ca, Mg, and Cr in traversing from early red and blue cathodoluminescence zones toward later green zones, typically with an increase in elements such as Li, Rb, Sr, Ti, Hf, Zr, and light rare earth elements (LREEs). Here we have replotted the data in a spidergram to show the entire pattern together (**Figure 8**). Individual samples show large variations in the concentrations of these trace elements as well as changes in $\delta^{18}\text{O}$ that can only be explained by multiple sources of fluid. Sorensen et al. (2006) suggest that the oxygen signature of the jadeite grains is mirrored by the fluid from which they grew, with three major sources reflected in the data: seafloor altered by seawater at low T , seafloor altered at higher T , and an “igneous” or “mantle” source. In a laser ablation inductively coupled plasma mass spectrometry study of jadeite and omphacite in P-type jadeitite from the Itoigawa-Omi district, Japan, Morishita et al. (2007) interpreted elevated large ion lithophile element (LILE) patterns, higher LREEs than HREEs, and positive anomalies of high field strength elements (HFSEs) relative to primitive mantle values; they suggested these findings were due to slab-derived fluids relatively rich in LILEs and HFSEs from interaction with subducted crust and serpentinized peridotites. Among elements measured in jadeite, only Li, Ni, Zr, Hf, and Nb exceed N-MORB values (Sun & McDonough 1989); when omphacite is considered, Sr and Cr are included in this list as well. This difference may point to the importance of crystal chemistry, given how trace elements enter crystal structures (e.g., Sr into Ca-rich omphacite, Li into Na-rich jadeite and omphacite), and of timing, as omphacite is late in jadeitites in general and is likely liberated late during serpentinization of peridotite.

By considering whole-rock analysis, some of the minor phases that are important in jadeitites are made obvious, although some signatures are consistent with the data above. A conspicuous feature of jadeitites from Myanmar and Guatemala is minor late-stage barium phases: cymrite (BaAl₂Si₂O₈•H₂O), celsian, banalsite, and hyalophane, as well as primary barian phengitic muscovite (Guatemala only). Some barian phases are found in jadeitite from California, Dominican



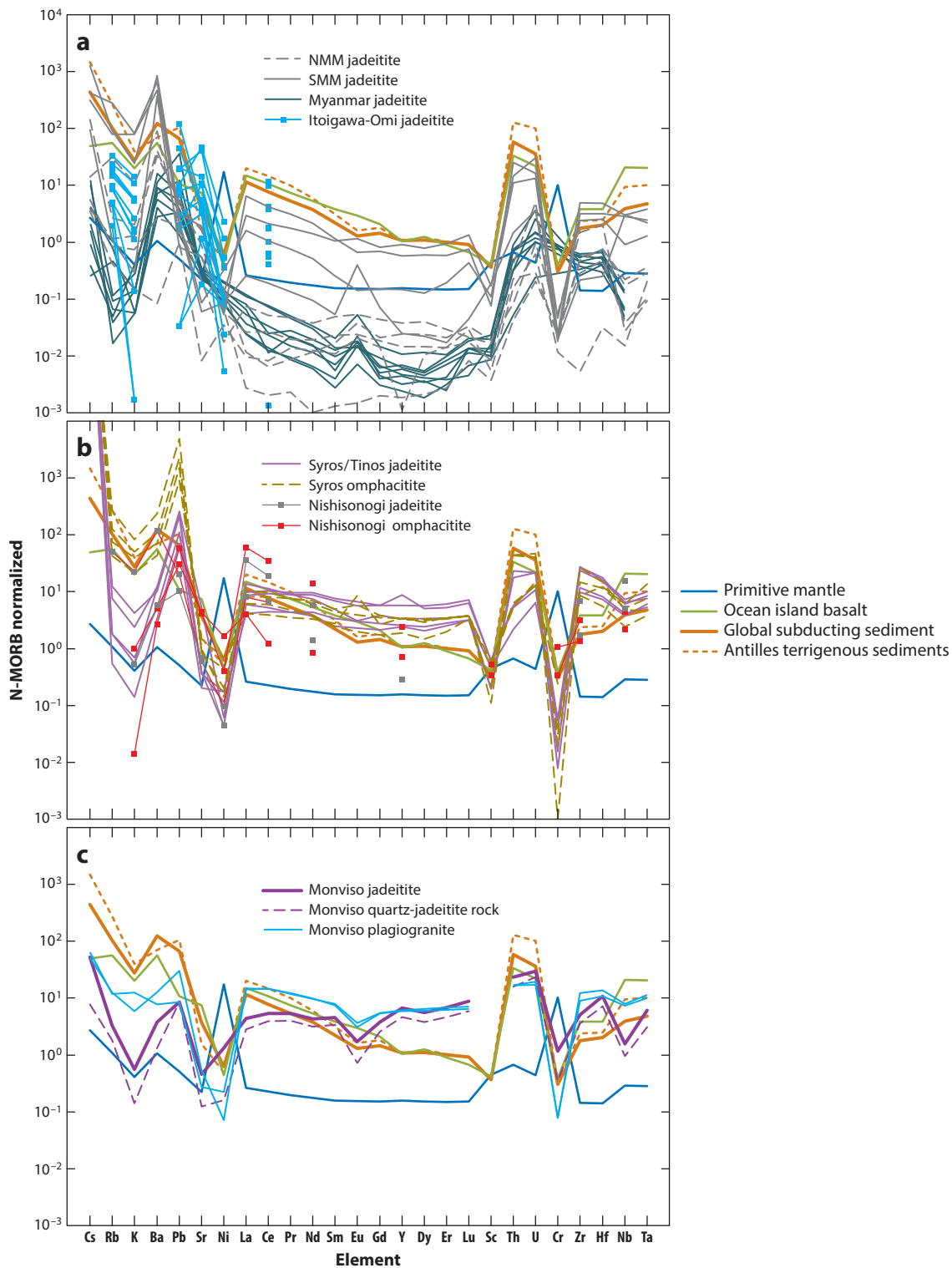
Republic, and Iran. Itoigawa-Omi jadeitite contains some celsian and Ba-rich K-spar but is known for its variety of strontium minerals such as itoigawaite [$\text{SrAl}_2\text{Si}_2\text{O}_7(\text{OH})_2 \bullet \text{H}_2\text{O}$], reingeite ($\text{Sr}_4\text{ZrTiSi}_4\text{O}_{22}$), and matsubaraite [$\text{Sr}_4\text{Ti}_5(\text{Si}_2\text{O}_7)_2\text{O}_8$]. Sr is enriched only in some calcic phases, such as lawsonite and zoisite, among Guatemalan jadeitites and is not very conspicuous in other jadeitites (see Harlow et al. 2011, 2014). These elements become conspicuous in the whole-rock data.

A limited amount of whole-rock analysis is available among the deposits that have been studied. Starting with jadeitite interpreted as fundamentally of P-type, the best data for samples from the Jade Mine Tract in Myanmar (Shi et al. 2008) show the enrichment of Ba but not Sr, as suspected from mineralogy, but also high Pb; somewhat high U ($>$ Th); low Rb, K, and Ti; and a depleted concave rare earth element (REE) pattern with a positive Eu anomaly, as shown in a field-strength-organized spider diagram normalized to N-MORB (**Figure 9**) (Sun & McDonough 1995). Simons et al. (2010) presented data on a single sample from the SMM, which has now been augmented by a comprehensive suite of jadeitites from various locales in both the SMM and NMM (G.E. Harlow, K.E. Flores & H.R. Marschall, manuscript in preparation). These data show some similarities with the Myanmar samples, with high Cs, Ba, and U, but otherwise show more variability in the range of values while sharing the same general pattern shape within each general source area, such as flatter more depleted REE patterns from the NMM versus asymmetric concave REE patterns straddling N-MORB values from the SMM [the pattern for sample MVE02-8-5 of Simons et al. (2010) shows the pronounced Eu anomaly not observed in a newer analysis, which suggests incomplete powder digestion in the former plus some Eu contamination, as no other samples show these characteristics; nonetheless, the data are included here]. Syros and Tinos jadeitites are categorized as a mixture of P-type and R-type formation, so interpreting the jadeitite compositions (Bröcker & Enders 2001) is problematic; nonetheless, the plotted data (**Figure 9**) are quite consistent with $\text{Ba} > \text{K} \approx \text{Sr}$; enriched U (\geq Th), Zr ($>$ Hf), Nb, and Ta; and flat, somewhat enriched REE patterns. Data from other P-type jadeitite sources [e.g., Itoigawa-Omi (Miyajima 1999) and Sorkhan, Iran (Oberhänsli et al. 2007)] are incomplete and thus are not plotted or considered. Among these P-type jadeitites, in spite of the differences, there are similarities in enriched Ba (\pm Pb or Sr) among the LILEs, U (\pm Th) compared with the REEs, and maybe Zr and Hf as well. Presumably, these features represent some combination of solute source, namely the subduction channel, and relative solubility in some unknown but large flux of hydrous fluid escaping from the channel.

The obvious candidates for the source of solutes in the fluids that precipitate P-type jadeitite are the components of the subducted oceanic crust, namely altered oceanic (basaltic) crust and the sediments overlying it. Simons et al. (2010) examined these possibilities in their study of Guatemala jadeitite and its constituents, with a focus on Li content and isotopic signature. They found that the Li concentration in jadeite (≤ 90 $\mu\text{g/g}$; somewhat less in jadeitite) was significantly greater than in N-MORB (3–6 $\mu\text{g/g}$), island arc basalt (5–10 $\mu\text{g/g}$), and altered oceanic crust (4–14 $\mu\text{g/g}$) and generally heavier (+2‰ to +7.5‰ $\delta^7\text{Li}$) compared with either jadeitite or eclogite (–5‰ to +5‰ $\delta^7\text{Li}$), such that a dehydration process with Rayleigh fractionation would not likely produce the observed signature in jadeitites. Sediments, in contrast, have both greater Li concentration and

Figure 8

Normal mid-ocean ridge basalt (N-MORB)-normalized trace element pattern for jadeite from jadeitites. (a) Guatemala (Sorensen et al. 2006, Harlow & Shi 2011). (b) Myanmar (Sorensen et al. 2006, Harlow & Shi 2011). (c) Itoigawa-Omi, Japan (Sorensen et al. 2006, Morishita et al. 2007, Harlow & Shi 2011). Normalized value and reference values are from Sun & McDonough (1989), McDonough & Sun (1995), and Plank & Langmuir (1998). Except for Sorensen et al.'s (2006) secondary ion mass spectrometry data, all data were collected by laser ablation inductively coupled plasma mass spectrometry.



lower $\delta^7\text{Li}$ compared with altered oceanic crust. Global subducted sediment (Plank & Langmuir 1998) or its Li-evaluated counterpart global Li mass-weighted sediment (43 $\mu\text{g/g}$ Li, $\delta^7\text{Li} = 3.01\text{‰}$; Chan et al. 2006), and particularly sediments with a continental source affinity, such as the Lesser Antilles (69.6 $\mu\text{g/g}$ Li), were selected for modeling a dehydration path to yield a fluid from which jadeitite could be crystallized. Moreover, sediments are a potential source of elevated LILEs and Th, U, Zr, Hf, Nb, and Ta, as can be seen in the whole-rock composition plots in **Figure 9**, to which global subducted sediment and Antillean terrigenous sediment values have been added. Li is not included in these plots because data on Li are available only from Myanmar jadeitites (a range of 26 to 35 $\mu\text{g/g}$ for six samples, and one sample at 5.8 $\mu\text{g/g}$); however, **Figure 8**, with just jadeite values, shows that Li is relatively high in jadeite in many, but not all, jadeitites.

The spider plots in **Figure 9** use field strength for elemental order to better gauge the role of crystal and fluid chemistry rather than igneous compatibility, and they manifest some features worth discussion. With the LILEs on the left, differentiated igneous rocks and clay-rich sediments generally show strong enrichments; however, jadeitites without mica are deficient in K compared with N-MORB, but less so than for Rb and particularly Cs in most cases where reported. Ba and Sr are discussed above with respect to mineralogy, but Pb is in the plots among the alkaline earth metals. Ba is a good signature of sediment, being a constituent of both pelagic and terrestrial detrital sediments (as shown in global subducted sediment data); it is conspicuously high in Guatemala, Myanmar, and Nishisonogi jadeitites and less so in Cyclades jadeitites and is nowhere reported as low. Sr is only modestly high in Itoigawa jadeitites and moderately low in Guatemala, Cyclades, Myanmar, and Sorkhan jadeitites, whereas Pb can be transitional between Sr and Ba (Guatemala, most Myanmar samples) or higher (Tone, Nishisonogi, two Myanmar samples). Ni and Cr are added as monitors of interactions with ultramafic, such as from release into the fluid upon completion of some serpentinization reactions; the values are very low where reported, suggesting little feedback during jadeitite crystallization. Th, U, Zr, and Hf are higher field strength elements that are generally considered less mobile. Jadeitites clearly show sympathetic variation within the pairs (Th and U; Zr and Hf) and varied concentrations, but following the pattern of either sediment or more evolved igneous rocks. These four elements are generally higher in the jadeitites from Cyclades and the SMM and lower in those from Myanmar and the NMM. The highest field strength pair is Nb and Ta, which are less well constrained but follow the trends of the previous four elements where measured, similar to sediment and ocean island basalt.

The REE patterns show considerable variation among jadeitites and make for an interesting comparison with sediment and oceanic igneous rocks. A characteristic of both sediments and evolved basaltic rocks (e.g., ocean island basalt) is an LREE-enriched pattern, decreasing with increasing atomic number (**Figure 9**). The same is true for global subducted sediment and the Antillean terrigenous sediment used in our comparison. In contrast, plagiogranite and trondhjemite, whether of suprasubduction zone or near-ridge origin, have generally flat and slightly

Figure 9

Normal mid-ocean ridge basalt (N-MORB)-normalized whole-rock minor trace element composition spidergrams for jadeitites. (a) Jadeitites from the Northern Motagua mélange (NMM) and Southern Motagua mélange (SMM) of Guatemala (Simons et al. 2010; G.E. Harlow, K.E. Flores & H.R. Marschall, manuscript in preparation); from Myanmar (Shi et al. 2008); and from Itoigawa-Omi, Japan (Miyajima 1999). (b) Jadeitites and omphacitites from Syros and Tinos, Greece (Bröcker & Enders 2001), and from Nishisonogi, Japan (Shigeno et al. 2012). (c) Jadeitites and associated quartz-jadeite rock and plagiogranite from Monviso, Italy (Compagnoni et al. 2012). Normalized value and reference values are from Sun & McDonough (1989), McDonough & Sun (1995), and Plank & Langmuir (1998). The order of the elements is based on field strength (ionic radius/ionic charge) for sixfold coordination rather than on melt incompatibility to better reflect crystal/solution chemistry. Radii are from Shannon (1976).

enriched patterns (more like N-MORB) with a minimal to small negative Eu anomaly. On a first-order basis, unless there is a multiminerall dependence on REE patterns that would affect patterns of solubilized REEs, the protolith pattern for solute (or just the protolith) probably represents that in solution. Thus, the REE pattern in jadeitite should resemble that in the solubilized source, offset by the capacity of REEs to substitute for Ca in jadeite, omphacite, or another Ca-bearing phase in jadeitite. The REE patterns in jadeitite that are LREE enriched (e.g., the SMM, Nishisonogi, and perhaps Myanmar) may owe that enrichment to sediment or ocean island basalt, whereas the flatter patterns (e.g., Cyclades and the NMM) may owe their patterns to (N-)MORB or plagiogranite. Itoigawa data are limited but appear to show both trends. Myanmar REE data are concave with a positive Eu anomaly.

The other half of understanding the REEs in jadeitite and their possible relationship to source or fluid composition is the mineral(s) that host(s) these elements. If allanite is the dominant host, the rock pattern will most likely be LREE enriched, whereas if monazite is dominant, the pattern may be flatter and convex. Jadeite itself plays a role in REE uptake to the extent that pure jadeitite does not offer a large crystallographic site for the REEs, but increased Ca content provides the site expansion in the average structure to accommodate more REEs; this is particularly evident in more calcic jadeitites (e.g., SMM jadeitite, Cyclades omphacitites; Bröcker & Enders 2001). Guatemala jadeitites typically contain more REE-rich clinozoisite and allanite than monazite, which may explain the pattern shape. Nishisonogi jadeitites are reported to contain allanite but not monazite. These are both consistent with REE patterns. The Myanmar jadeitites have rare allanite but very depleted REE patterns, so connecting the shape to a mineral or solute source remains difficult.

In conclusion, the enrichments in the LILEs Ba, Pb, and perhaps Sr, as well as in Li, are consistent with crystallization from fluids derived from a sediment-rich source and probably controlled in the jadeitite by compatibility in jadeite (for Li) and in minor phases such as the Ba- or Sr-silicates, epidote-group minerals, or mica (for the LILEs). Without saturation of K-mica, K is usually depleted. Enrichments in more “immobile” elements such as Th, U, Zr, Hf, Nb, and Ta appear to correlate with an enriched source, such as sediment, but how this transport occurs must relate to solubilities at *HP/LT* conditions and fluid flux, addressed below. This is not to suggest that the main bolus of solutes—Na, Al, and Si—does not come from altered oceanic crust, as Simons et al. (2010) have suggested, because clearly its dehydration must be involved in producing the hydrous fluid indicated in the jadeitite formation process.

4.3. Protolith for R-Type Jadeitite Samples

R-type jadeitites have been interpreted as desilicified plagiogranite or some other felsic protolith entrained in a mélangé or precipitated in metabasite without direct contact with ultramafic. The best data are for a jadeitite from Vallone Bulè, western Italian Alps, which Compagnoni et al. (2012) interpreted as the desilicified cortex of a quartz jadeitite block in a basal serpentinite unit of the Monviso massif; they interpreted the block as a metaplagiogranite originally formed in a near-ridge environment. The whole-rock data, replotted in **Figure 9c**, illustrate one of the bases for this interpretation: The patterns are very similar. The distinguishing feature from the jadeitite analysis is the somewhat enriched, relatively flat REE pattern; additionally, all of the related rocks show negative Eu anomalies, which is distinctive compared with most P-type jadeitites. The only other data for jadeitite interpreted as R-type are those of Shigeno et al. (2012) for Nishisonogi jadeitites that were suggested to be metaplagiogranite. Although only limited REE data are available, rather than resembling the Monviso results, they indicate an LREE-enriched/HREE-depleted trend (**Figure 9**). This pattern is not much closer to the flatter pattern of suprasubduction zone

trondhjemite-tonalite-diorite as exemplified by the data of Shervais (2008). The greatest similarity is to the pattern of a sediment signature of global subducted sediment or of continentally derived sediment of the Caribbean Antilles, as suggested by Simons et al. (2010) for the solute host of Guatemalan jadeitite.

4.4. Fluid Properties and Mineral Solubilities at HP/LT Conditions

Understanding the nature of subduction fluids derived from dehydration reactions has been enhanced by the work of Manning (1998, 2004), which showed that, at conditions of the blueschist-to-eclogite transition, the fluid produced would be enriched not only in silica and Na but also in Al. Manning also suggested the influence of the overriding mantle reacting with excess silica in the fluid to saturate an NaAl-silicate phase. Wohlers et al. (2011) experimentally evaluated the solubility of albite and jadeite in H₂O with paragonite and quartz at conditions consistent with subduction channels (500°C and 600°C; 1–2.25 GPa). The experiments show a strong positive effect of both *P* and *T* upon the solubility of each element in the presence of albite, but this effect decreases with *P* in the stability field of jadeite. Moreover, the solubilities are greater than predicted from extant thermodynamic data, which the authors attribute to an unaccounted solute species involving all three elements. Bulk solubility with excess Qz at the Ab-Jd-Qz equilibrium is ~3.3 wt% (500°C and 1.52 GPa from their experiments), clearly a considerable solute content relevant to jadeitite formation. Moreover, as the authors point out, a fluid ascending isothermally will dissolve components in this simple system until reaching the Ab-Jd-Qz equilibrium, at which point crystallization will occur; this may be an important aspect of jadeitite formation, although it needs to be evaluated in a much more complicated chemical system that includes the role of interactions with ultramafic.

Two important considerations for interpreting jadeitite formation are the properties of H₂O at HP/LT conditions and the amount of fluid available for transport. The solute carrying capacity of hydrous fluid at HP/LT conditions changes as both the dipole moment and dielectric constant of H₂O increase, changing a polar solvent to an ionic solvent (e.g., Galvez et al. 2013, Pan et al. 2013, Angiboust et al. 2014) and increasing the solubility of many solids. As pointed out above in the work of Wohlers et al. (2011), the solubilities of multiple elements, particularly important with alkali available to combine with high field strength cations, probably make even the most immobile elements enter a hydrous fluid in greater concentrations at subduction channel conditions than along shallower geotherms. Next is the issue of the amount of water expelled by dehydration of the subducting slab, which includes amphiboles with 1–2 wt% H₂O and phyllosilicates with up to 12 wt% H₂O. If these fluids can carry several weight percent of dissolved solutes, the required carrying capacity for the trace elements shown in **Figure 9**, which varies from ~5,000 µg/g for Ba to 500 µg/g for Zr to 7 µg/g for Nb, need not be large if the fluid-to-rock ratio is also large [probably in the neighborhood of 100 based on the fluid/mineral partitioning compiled by Sorensen et al. (2006)]. Jadeitites indicate that this transport process is indeed happening, and that the fluid does not terminate with the crystallization of jadeitite but rather helps saturate the mantle wedge sponge effect for water and likely continues to feed flux melting processes at higher temperatures.

4.5. When in the Life of a Subduction Zone Mélange Do Jadeitites Form?

The timing of jadeitite crystallization in the subduction process is an important topic that has received increasing attention with the availability of U-Pb dating of zircon from jadeitites. Serpentine mélanges themselves can have complicated evolutions, with incorporation of metasediments and metabasites during active subduction prior to whatever event ultimately drives exhumation

(e.g., Gerya 2011). The issues in interpreting jadeitite ages are (*a*) whether the dated zircons are inherited from a protolith in some aspect of an R-type origin and thus not indicative of the jadeite-forming event and (*b*) whether they form during active subduction well before exhumation or form upon termination of active subduction and the transition to exhumation. In the latter case, termination is typically correlated with peak metamorphism in the eclogites that are associated with the youngest and coldest events recorded by eclogites within the mélangé. Understanding what geochronological measurements actually record is important in this context and is another fundamental aspect to unraveling these fossil subduction systems.

Tsujimori & Harlow (2012) reviewed the available literature, and a revision of their results is given in **Table 2** [citations are provided for new additions; see the review by Tsujimori & Harlow (2012) for the rest]. Part of the revision derives from new zircon dating from Guatemala (Yui et al. 2012, Flores et al. 2013) and Myanmar (Yui et al. 2013). The dates show that jadeitite may be significantly older than the peak metamorphic age of rocks derived and exhumed from the subducted slab. Examples of this are the NMM and SMM, where primary zircon in jadeitite is as much as 25 and 22 Ma older than eclogite dates, respectively; the Itoigawa and Osayama belts, where it is more than 100 Ma older (Tsujimori et al. 2005); the Polar Urals, where it is ~38–28 Ma older (Shatsky et al. 2000; Glodny et al. 2003, 2004); and the Río San Juan complex mélangé, where it is 20–10 Ma older. The Jade Mine Tract had been considered an example, with as much as 78 Ma difference in age (Shi et al. 2008, Qiu et al. 2009); however, if Yui et al. (2013) are correct, the older zircon dates from jadeitite represent inherited ages, with the youngest ages, 77 ± 3 Ma, being comparable to the peak metamorphic age. Given the poor sampling from this area and the need for systematic study of both jadeitite and other HP/LT rocks, the final word is probably not in.

Among the above interpretations, there have been disagreements as to whether the zircons in jadeitite are inherited (Fu et al. 2010 for Guatemala jadeitite and Yui et al. 2013 for Myanmar jadeitite) or primary (Yui et al. 2010 and Flores et al. 2013 for Guatemala jadeitite and Shi et al. 2008 and Qiu et al. 2009 for Myanmar jadeitite). For the former position, the authors argue on the basis of Th/U ratios, REE characteristics, and/or older cores; for the latter position, the authors argue on the basis of trace elements and/or inclusions in zircon that are indicative of a nonigneous origin—minerals consistent with jadeitite or hydrous fluid inclusions. We do not go further into the details here, but some of the arguments are unlikely to be resolved without more data in these and probably other cases. Moreover, the data on the counterpart metabasites are absent for Myanmar and subject to further refinement for Guatemala.

Then there are cases where the jadeitite and peak metamorphism ages are similar: Sierra del Convento, with no more than 1–10 Ma difference, and Syros, with equivalent 80 Ma ages. Clearly, vastly older ages imply that jadeitite is sequestered from foundering with the subducting slab through formation in the mantle wedge and provide evidence for continued growth (e.g., Guatemala; Flores et al. 2013) until initiation of exhumation. The examples of contemporary ages may require a short-lived jadeitite formation process or poor preservation (sampling?). Our interpretation is that indeed some, if not most, jadeitites are formed and stored prior to exhumation, as recorded by peak metamorphic ages of other HP/LT blocks, although inheritance of protolith ages in some R-type jadeitite is possible (though not demonstrated). Until more radiometric dating is performed, perhaps with more minerals and isotopic systems, the debate will continue. One of the next conundrums is an understanding of the long-term preservation or storage of old jadeitite (e.g., Polar Urals or southwest Japan) without retrogression to low-pressure assemblages. There is much to learn from these rare and valuable rocks.

The dating of the R-type jadeitites is largely consistent with their interpreted origin: older inherited zircon cores and younger rims, consistent with the metamorphic history of other rocks

and the timing of the jadeite metasomatism in the incorporating mélanges (Yui et al. 2012 for Tone jadeitite and Schertl et al. 2012 and Hertwig et al. 2013 for Río San Juan complex jadeitite).

5. JADEITITE SIGNIFICANCE IN THE SUBDUCTION FACTORY

Jadeitites, despite not being as common (or as commonly recognized) as other lithologies, are an important member of the *HP/LT* rocks preserved from subduction channels in exhumed serpentinite-matrix mélanges. As products of channel fluid precipitation (P-type) and metasomatism (R-type), they preserve a record of the fluid from their loci of crystallization. That most P-type jadeitites are or were hosted by serpentinite demonstrates the transfer of dissolved slab (and sediment) content into the mantle wedge, which makes them important boundary value samples for fluid infiltration during arc formation. They appear to provide strong evidence for the sponge effect of mantle wedge peridotite described by Deschamps et al. (2010), in part to facilitate supersaturation of the fluid in jadeitite minerals and in part to change the $\text{Si} > \text{Na,Al}$ in *HP* fluid (as indicated in the experiments by Wohlers et al. 2011) with the silica consumption in the reaction of peridotite (modal olivine $>$ orthopyroxene) to form antigorite serpentinite without brucite (e.g., Harlow et al. 2006). Any complete model of the subduction factory needs to incorporate the role played by and restrictions placed on the process of jadeitite formation and to explain the distribution of jadeitites in the geological record. In this respect, we are still in the early days.

6. JADEITITE AS A PETROTECTONIC INDICATOR

The temporal distribution of *HP/LT* and ultrahigh-pressure (*UHP*) metamorphic rocks provides a key constraint on when subduction-like geothermal gradients existed, or at least when rocks cooked in these environments were returned to the surface. Stern et al. (2013) recognized jadeitite as a key petroTECTONIC indicator for plate tectonics and proposed the term plate tectonic gemstones for jadeitite as the subduction zone gemstone and ruby (gem corundum of metamorphic origin) as the continental collision zone gemstone. The oldest occurrences of jadeitite are Early Paleozoic (**Figure 10**), suggesting that subduction zone thermal structures did not evolve toward the necessary *LT* conditions needed for jadeite and blueschist formation until that time. Alternatively, aspects of these geological records may have been eroded from older crust, or the assemblages may have reequilibrated to ones more consistent with crustal geotherms (relatively higher *T* or lower *P*). Compared with the secular trend of other Phanerozoic petroTECTONIC indicators for subduction tectonics, the bimodal temporal distribution of jadeitites might have a hidden geological meaning. A long hiatus from 400 to 200 Ma suggests no general correlation among exhumations of jadeitite and *HP/LT* metamorphic belts, instead showing a good correlation with the ophiolite pulse. Exhumation of *HP/LT* metamorphic rocks is episodic, and exhumation or preservation of a jadeite-bearing mélange complex is more likely accidental. Seafloor spreading presumably is a continuous event, and therefore so are subduction and consequently jadeitite formation in the mantle wedge. Intensified study of jadeitite-bearing mélange complexes and associated suprasubduction zone ophiolite components should allow a better understanding of the geodynamics of mantle wedge evolution.

7. TOPICS FOR FUTURE ATTENTION

Even though subduction zone-related serpentinite mélanges and *HP/LT* belts are widespread around ancient and modern convergent plate tectonic boundaries (e.g., Maruyama et al. 1996, Tsujimori & Ernst 2014), jadeitite occurrences are rare. What is the reason for this discordance

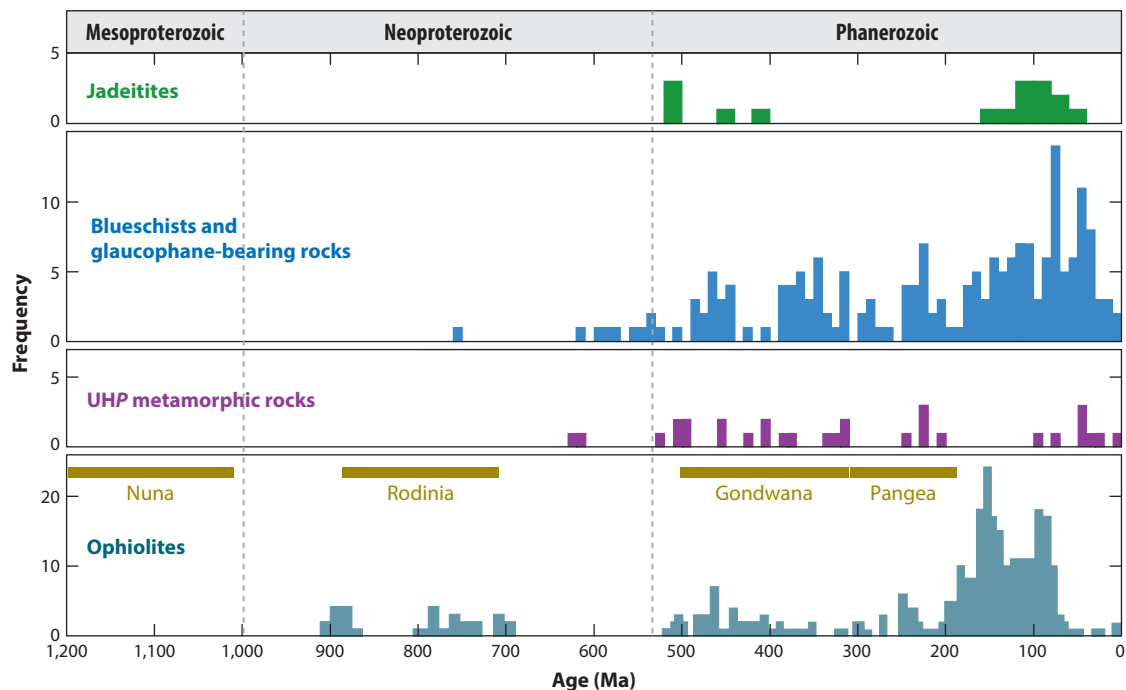


Figure 10

Histograms showing ages of jadeitite, blueschists and glaucophane-bearing eclogites (Tsuji-mori & Ernst 2014), ultrahigh-pressure (UHP) metamorphic rocks (Liou et al. 2014), and ophiolites (Dilek 2003). Supercontinent cycles are from Bradley (2011).

with the observed record? If the model of fluid crystallization is approximately correct, jadeitite should be a common product of subduction. Is the model wrong, or is the lack due to some aspect of the exhumation process and its geodynamics? Several jadeitite occurrences are distributed on present-day transforms or lateral faults: Sagaing fault in Myanmar, Motagua fault in Guatemala, and the Itoigawa-Shizuoka tectonic lineament in central Japan. This characteristic has been cited previously, and a special role for so-called transtensional settings has been suggested (Harlow et al. 2014); however, no evaluation has been carried out.

Trace element signatures of jadeitites hold out some hope for identifying both the original characteristics of the package of sediment and altered oceanic crust sampled by the crystallizing fluid in the case of P-type jadeitites and of the actual protolith in the case of R-type jadeitites. Clearly, the complexity of the fluids, as shown by Sorensen et al. (2006), and the possibility of further metasomatic activity make these interpretations less certain. Zircons in jadeitite, although typically small, have been used to argue for both P-type and R-type origin. A larger array of trace element analyses of jadeitite zircons should help resolve the origin and evolution of jadeitites worldwide, as well as the issue of timing relationships between jadeitite formation and subduction/exhumation history.

DISCLOSURE STATEMENT

The authors are not aware of any affiliations, memberships, funding, or financial holdings that might be perceived as affecting the objectivity of this review.

ACKNOWLEDGMENTS

This research was supported by grants from the US National Science Foundation (EAR 0309116 and 1119403) awarded to G.E.H. and in part by the MEXT/JSPS KAKENHI (24403010) awarded to T.T. This manuscript was reviewed and improved by Raymond Jeanloz. We thank him as well as *Jaderos* (Virginia Sisson, Hannes Brueckner, Horst Marschall, Kennet Flores, and Céline Martin) for support and helpful feedback.

LITERATURE CITED

- Angiboust S, Pettke T, de Hoog CJ, Caron B, Oncken O. 2014. Channelized fluid flow and eclogite-facies metasomatism along the subduction shear zone. *J. Petrol.* 55:883–916
- Birch F, LeCompte P. 1960. Temperature-pressure plane for albite composition. *Am. J. Sci.* 258:209–17
- Bleek AWG. 1908. Jadeite in the Kachin Hills, Upper Burma. *Rec. Geol. Surv. India* 36:254–85
- Bosc EA. 1971. *Geology of the San Agustín Acasaguastlán Quadrangle and Northeastern part of El Progreso Quadrangle, Guatemala*. PhD Thesis, Rice Univ., Houston, TX
- Bradley DC. 2011. Secular trends in the geologic record and the supercontinent cycle. *Earth-Sci. Rev.* 108:16–33
- Bröcker M, Enders M. 2001. Unusual bulk-rock compositions in eclogite-facies rocks from Syros and Tinos (Cyclades, Greece): implications for U-Pb zircon geochronology. *Chem. Geol.* 175:581–603
- Bröcker M, Keasling A. 2006. Ionprobe U-Pb zircon ages from the high-pressure/low-temperature mélange of Syros, Greece: age diversity and the importance of pre-Eocene subduction. *J. Metamorph. Geol.* 24:615–31
- Buffon G-LL. 1749. *Histoire Naturelle, Générale et Particulière, avec la Description du Cabinet du Roi*. Paris: Imprim. R.
- Buffon G-LL. 1783–1788. *Histoire Naturelle des Minéraux*. Paris: Imprim. R.
- Cárdenas-Párraga J, García-Casco A, Núñez-Cambra K, Rodríguez-Vega A, Blanco-Quintero IF, et al. 2010. Jadeitite occurrence from the Sierra del Convento mélange (eastern Cuba). *Bol. Soc. Geol. Mex.* 62:199–205
- Carpenter MA. 1981. Time-temperature-transformation (TTT) analysis of cation disordering in omphacite. *Contrib. Mineral. Petrol.* 78:433–40
- Chan LH, Leeman WP, Plank T. 2006. Lithium isotopic composition of marine sediments. *Geochim. Geophys. Geosyst.* 7:2005GC001202
- Chhibber HL. 1934. *The Mineral Resources of Burma*. London: MacMillan
- Coggon R, Holland TJB. 2002. Mixing properties of phengitic micas and revised garnet-phengite thermobarometers. *J. Metamorph. Geol.* 20:683–96
- Coleman RG. 1961. Jadeite deposits of the Clear Creek area, New Idria district, San Benito County, California. *J. Petrol.* 2:209–47
- Coleman RG. 1971. Plate tectonic emplacement of upper mantle peridotites along continental edges. *J. Geophys. Res.* 76:1212–22
- Coleman RG. 1980. Tectonic inclusions in serpentinite. *Arch. Sci.* 33:89–102
- Compagnoni R, Rolfo F. 2003. First report of jadeitite from the Monviso meta-ophiolite, Western Alps. *Geotitalia* 4:205–6
- Compagnoni R, Rolfo F, Castelli D. 2012. Jadeitite from the Monviso meta-ophiolite, western Alps: occurrence and genesis. *Eur. J. Mineral.* 24:333–43
- da Silva ZCG. 1967. *Studies on jadeites and albites from Guatemala*. MA Thesis, Rice Univ., Houston, TX
- da Silva ZCG. 1970. Origin of albitites from eastern Guatemala. *Bol. Serv. Geol. Minas* 22:23–32
- Dale J, Powell R, White RW, Elmer FL, Holland TJB. 2005. A thermodynamic model for Ca-Na clin amphiboles in Na₂O-CaO-FeO-MgO-Al₂O₃-SiO₂-H₂O-O for petrological calculations. *J. Metamorph. Geol.* 23.8:771–91
- Damour AA. 1846. Analyses du jade oriental. *Ann. Chim. Phys.* 16:469–74
- Damour AA. 1881. Nouvelles analyses sur la jadeite et sur quelques roches sodifères. *Bull. Soc. Fr. Min. Crist.* 4:157–64

- de Capitani C, Petrakakis K. 2010. The computation of equilibrium assemblage diagrams with Theriak/Domino software. *Am. Mineral.* 95:1006–16
- de Roever WP. 1955. Genesis of jadeite by low-grade metamorphism. *Am. J. Sci.* 253:283–98
- Deschamps F, Godard M, Guillot S, Hattori K. 2013. Geochemistry of subduction zone serpentinites: a review. *Lithos* 178:96–127
- Deschamps F, Guillot S, Godard M, Chauvel C, Andreani M, Hattori K. 2010. In situ characterization of serpentinites from forearc mantle wedges: timing of serpentinization and behavior of fluid-mobile elements in subduction zones. *Chem. Geol.* 269:262–77
- Dilek Y. 2003. Ophiolite pulses, mantle plumes and orogeny. *Geol. Soc. Spec. Publ.* 218:9–19
- Dilek Y, Furnes H. 2014. Ophiolites and their origin. *Elements* 10:93–100
- Dobretsov NL. 1984. Problem of the jadeite rocks, associating with ophiolites. *Mineral. Slov.* 16:3–12
- Dobretsov NL, Ponomareva LG. 1965. Comparative characteristics of jadeite and associated rocks from Polar Ural and Prebalkhash region, transl. JE Agrell, 1968. *Int. Geol. Rev.* 10:221–79 (from Russian)
- Draper G, Nagle F, Renne PR. 1991. Geology, structure, and tectonic development of the Rio San Juan Complex, northern Dominican Republic. *Geol. Soc. Am. Spec. Pap.* 262:77–96
- Ernst WG. 1970. Tectonic contact between the Franciscan Mélange and the Great Valley Sequence—crustal expression of a Late Mesozoic Benioff Zone. *J. Geophys. Res.* 75:886–901
- Evans BW. 2004. The serpentinite multisystem revisited: Chrysotile is metastable. *Int. Geol. Rev.* 46:479–506
- Fishman AM. 2006. *Gems in the North Ural and Timan.* Syktyvkar, Russ.: Geoprint
- Flores KE, Martens U, Harlow GE, Brueckner HK, Pearson N. 2013. Jadeitite formed during subduction: in situ zircon geochronology constraints from two different tectonic events in the Guatemala Suture Zone. *Earth Planet. Sci. Lett.* 371–72:67–81
- Foshag WF. 1957. Mineralogical studies on Guatemalan jade. *Smithson. Misc. Collect.* 135:4307
- Foshag WF, Leslie R. 1955. Jadeite from Manzanal, Guatemala. *Am. Antiq.* 21:81–83
- Fu B, Paul B, Cliff J, Bröcker M, Bulle F. 2012. O-Hf isotope constraints on the origin of zircons in high-pressure mélange blocks and associated matrix rocks from Tinos and Syros, Greece. *Eur. J. Mineral.* 24:277–87
- Fu B, Valley JW, Kita NT, Spicuzza MJ, Paton C, et al. 2010. Origin of zircons in jadeitite. *Contrib. Mineral. Petrol.* 159:769–80
- Galvez ME, Martinez I, Beyssac O, Benzerara K, Agrinier P, Assayag N. 2013. Metasomatism and graphite formation at a lithological interface in Malaspina (Alpine Corsica, France). *Contrib. Mineral. Petrol.* 166:1687–708
- García-Casco A, Rodríguez Vega A, Cárdenas Párraga J, Iturralde-Vinent MA, Lázaro C, et al. 2009. A new jadeitite jade locality (Sierra del Convento, Cuba): first report and some petrological and archaeological implications. *Contrib. Mineral. Petrol.* 158:1–16
- Gerya TV. 2011. Future directions in subduction modeling. *J. Geodyn.* 52:344–78
- Giaramita MJ, Sorensen SS. 1994. Primary fluids in low-temperature eclogites: evidence from two subduction complexes (Dominican Republic, and California, USA). *Contrib. Mineral. Petrol.* 117:279–92
- Glodny J, Austrheim H, Molina JF, Rusin A, Seward D. 2003. Rb/Sr record of fluid-rock interaction in eclogites: the Marun-Keu complex, Polar Urals, Russia. *Geochim. Cosmochim. Acta* 67:4353–71
- Glodny J, Pease V, Montero P, Austrheim H, Rusin AI. 2004. Protolith ages of eclogites, Marun-Keu Complex, Polar Urals, Russia: implications for the pre- and early Uralian evolution of the northeastern European continental margin. *Geol. Soc. Mem.* 30:87–105
- Green ECR, Holland TJB, Powell R. 2007. An order-disorder model for omphacitic pyroxenes in the system jadeite-diopside-hedenbergite-acmite, with applications to eclogite rocks. *Am. Mineral.* 92:1181–89
- Harlow GE. 1994. Jadeitites, albitites and related rocks from the Motagua Fault Zone, Guatemala. *J. Metamorph. Geol.* 12:49–68
- Harlow GE, Davies HL, Summerfield GR, Matisoo-Smith E. 2012a. *Archaeological jade mystery solved using a 119-year-old rock collection specimen.* Presented at AGU Fall Meet., Dec. 3–7, San Francisco, CA. Abstr. ED41E-0706
- Harlow GE, Flores KE. 2011. Jadeite jade: origin, sources, varieties and exploration. In *Proc. Int. Symp. Jade*, ed. HAO Weicheng, pp. 13–22. Beijing: Peking Univ.

- Harlow GE, Price NA, Tsujimori T. 2006. *Serpentinites of the Motagua fault zone, Guatemala: a mineralogical assessment*. Presented at 19th Gen. Meet. Int. Mineral. Assoc., July 23–28, Kobe, Jpn. Abstr. P19-17
- Harlow GE, Shi G. 2011. An LA-ICP-MS study of lavender jadeite from Burma, Guatemala, and Japan. *Gems Gemol.* 47:116–17 (Abstr.)
- Harlow GE, Sisson VB, Sorensen SS. 2011. Jadeitite from Guatemala: distinctions among multiple occurrences. *Acta Geol.* 9:363–87
- Harlow GE, Sorensen SS. 2005. Jade (nephrite and jadeitite) and serpentinite: metasomatic connections. *Int. Geol. Rev.* 47:113–46
- Harlow GE, Sorensen SS, Sisson VB. 2007. Jade. *Mineral. Assoc. Can. Short-Course Ser.* 37:207–54
- Harlow GE, Sorensen SS, Sisson VB, Shi G. 2014. The geology of jade deposits. *Mineral. Assoc. Can. Short-Course Ser.* 44:305–74
- Harlow GE, Summerfield GR, Davies HL, Matisoo-Smith L. 2012b. A jade gouge from Emirau Island, Papua New Guinea (Early Lapita context: 3300 BP): a unique jadeitite. *Eur. J. Mineral.* 24:391–99
- Hertwig A, McClelland WC, Kitajima K, Schertl HP, Maresch WV, Valley JW. 2013. *Geochronology, geochemistry and oxygen isotopes of zircon in a concordant jadeitite layer and its blueschist host (Rio San Juan Complex, Dominican Republic)*. Presented at 10th Int. Eclogite Conf., Sept. 2–10, Courmayeur, Italy. Abstr. 52
- Hirth G, Guillot S. 2013. Rheology and tectonic significance of serpentinite. *Elements* 9:107–13
- Holland TJB, Powell R. 1998. An internally consistent thermodynamic dataset for phases of petrological interest. *J. Metamorph. Geol.* 16:309–43
- Hughes RW, Galibert O, Bosshart G, Ward F, Oo T, et al. 2000. Burmese jade: the inscrutable gem. *Gems Gemol.* 36:2–26
- Isacks B, Oliver J, Sykes LR. 1968. Seismology and the new global tectonics. *J. Geophys. Res.* 73:5855–99
- Johnson CA, Harlow GE. 1999. Guatemala jadeitites and albitites were formed by deuterium-rich serpentinizing fluids deep within a subduction zone. *Geology* 27:629–32
- Kelemen PB, Matter J, Streit EE, Rudge JF, Curry WB, Blusztajn J. 2011. Rates and mechanisms of mineral carbonation in peridotite: natural processes and recipes for enhanced, in situ CO₂ capture and storage. *Annu. Rev. Earth Planet. Sci.* 39:545–76
- Knippenberg S, Rodríguez Ramos R, Schertl HP, Maresch WV, Hertwig A, et al. 2012. *The manufacture and exchange of jadeitite celt in the Caribbean*. Presented at 1st Eur. Mineral. Conf., Sept. 2–6, Frankfurt, Ger. Abstr. EMC2012-400
- Kunugiza K, Goto A. 2010. Hydrothermal activity of the Hida-Gaien belt indicating initiation of subduction of proto-Pacific plate in ca. 520 Ma. *J. Geogr.* 119:279–93
- Lázaro C, García-Casco A, Rojas Agramonte Y, Kröner A, Neubauer F, Iturralde-Vinent M. 2009. Fifty-five-million-year history of oceanic subduction and exhumation at the northern edge of the Caribbean plate (Sierra del Convento mélange, Cuba). *J. Metamorph. Geol.* 27:19–40
- Liou JG, Tsujimori T, Yang JS, Zhang RY, Ernst WG. 2014. Recycling of crustal materials through study of ultrahigh-pressure minerals in collisional orogens, ophiolites, and mantle xenoliths: a review. *J. Asian Earth Sci.* 96:386–420
- Liou JG, Tsujimori T, Zhang RY, Katayama I, Maruyama S. 2004. Global UHP metamorphism and continental subduction/collision: the Himalayan model. *Int. Geol. Rev.* 46:1–27
- Manning CE. 1998. Fluid composition at the blueschist-eclogite transition in the model system Na₂O-MgO-Al₂O₃-SiO₂-H₂O-HCl. *Schweiz. Mineral. Petrogr. Mitt.* 78:225–42
- Manning CE. 2004. The chemistry of subduction-zone fluids. *Earth Planet. Sci. Lett.* 223:1–16
- Maresch W, Grevel C, Stanek KP, Schertl HP, Carpenter M. 2012. Multiple growth mechanisms of jadeite in Cuban metabasite. *Eur. J. Mineral.* 24:217–35
- Martens U, Brueckner HK, Mattinson CG, Liou JG, Wooden JL. 2012. Timing of eclogite-facies metamorphism of the Chuacús complex, Central Guatemala: record of Late Cretaceous continental subduction of North America's sialic basement. *Litbos* 146–47:1–10
- Maruyama S, Liou JG, Terbayashi M. 1996. Blueschists and eclogites of the world and their exhumation. *Int. Geol. Rev.* 38:485–594
- McBirney AR, Aoki KI, Bass M. 1967. Eclogites and jadeite from the Motagua fault zone, Guatemala. *Am. Mineral.* 52:908–18

- McDonough WF, Sun SS. 1995. The composition of the Earth. *Chem. Geol.* 120:223–53
- Meng F, Makeyev AB, Yang JS. 2011. Zircon U–Pb dating of jadeitite from the Syum–Keu ultramafic complex, Polar Urals, Russia: constraints for subduction initiation. *J. Asian Earth Sci.* 42:596–606
- Miyajima H. 1999. *Bulk chemistry of jades from the Itoigawa-Omi district*. Presented at Annu. Meet. Jpn. Assoc. Mineral. Petrol. Econ. Geol., Sept. 24–26, Mito, Jpn. Abstr. 170
- Miyashiro A, Banno S. 1958. Nature of glaucophanitic metamorphism. *Am. J. Sci.* 256:97–110
- Mori Y, Orihashi Y, Miyamoto T, Shimada K, Shigeno M, Nishiyama T. 2011. Origin of zircon in jadeitite from Nishisonogi metamorphic rocks, Kyushu, Japan. *J. Metamorph. Geol.* 29:673–84
- Morishita T, Arai S, Ishida Y. 2007. Trace element compositions of jadeite (+omphacite) in jadeitites from the Itoigawa–Ohmi district, Japan: implications for fluid processes in subduction zones. *Island Arc* 16:40–56
- Mottana A. 2012. Mineral novelties from America during Renaissance: the “stones” in Hernández’ and Sahagún’s treatises (1576–1577). *Rend. Lincei* 23:165–86
- Nagel TJ, Hoffmann JE, Munker C. 2012. Generation of Eoarchean tonalite-trondhjemite-granodiorite series from thickened mafic arc crust. *Geology* 40:375–78
- Newton MS, Kennedy GC. 1968. Jadeite, analcime, nepheline and albite at high temperatures and pressures. *Am. J. Sci.* 266:728–35
- Nicolas A, Jackson M. 1982. High temperature dikes in peridotites: origin by hydraulic fracturing. *J. Petrol.* 23:568–82
- Oberhänsli R, Bousquet R, Moinzadeh H, Moazzen M, Arvin M. 2007. The field of stability of blue jadeite: a new occurrence of jadeitite from Sorkhan, Iran, as a case study. *Can. Mineral.* 45:1705–13
- Pan D, Spanu L, Harrison B, Sverjensky DA, Galli G. 2013. Dielectric properties of water under extreme conditions and transport of carbonates in the deep Earth. *PNAS* 110:6646–50
- Peacock S. 2001. Are the lower planes of double seismic zones caused by serpentine dehydration in subducting oceanic mantle? *Geology* 29:299–302
- Plank T, Langmuir CH. 1998. The chemical composition of subducting sediment and its consequences for the crust and mantle. *Chem. Geol.* 145:325–94
- Qi M, Xiang H, Zhang ZM, Zhong ZQ. 2014. Zircon U–Pb ages of Myanmar jadeitite and constraint on the fluid in subduction zone of the Neo-Tethys. *Acta Petrol. Sin.* 30:2279–86
- Qiu ZL, Wu FY, Yang SF, Zhu M, Sun JF, Yang P. 2009. Age and genesis of the Myanmar jadeite: constraints from U–Pb ages and Hf isotopes of zircon inclusions. *Chin. Sci. Bull.* 54:658–68
- Robertson EC, Birch F, MacDonald GJF. 1957. Experimental determination of jadeite stability relations to 25,000 bars. *Am. J. Sci.* 255:115–37
- Roy R, Tuttle OF. 1956. Investigations under hydrothermal conditions. *Phys. Chem. Earth* 1:138–80
- Schertl HP, Hertwig A, Knippenberg S, Maresch W, Speich L, et al. 2014. Jade artefacts from the Playa Grande site, Dominican Republic: mineralogical characterization and archeological implications. In *21st Gen. Meet. Int. Mineral. Assoc. (IMA) Abstr. Vol.*, ed. D Chetty, L Andrews, J de Villiers, R Dixon, P Nex, et al., p. 202. Johannesburg: Geol. Soc. S. Afr./Mineral. Assoc. S. Afr.
- Schertl HP, Maresch WV, Stanek KP, Hertwig A, Krebs M, et al. 2012. New occurrences of jadeitite, jadeite quartzite and jadeite-lawsonite quartzite in the Dominican Republic, Hispaniola: petrological and geochronological overview. *Eur. J. Mineral.* 24:199–216
- Schulze DJ, Flemming RL, Shepherd PHM, Helmstaedt H. 2014. Mantle-derived gyaunaite in a Cr-omphacite xenolith from Moses Rock diatreme, Utah. *Am. Mineral.* 99:1277–83
- Shannon RD. 1976. Revised effective ionic radii and systematic studies of interatomic distances in halides and chalcogenides. *Acta Crystallogr. A* 32:751–57
- Shatsky VS, Simonov VA, Yagoutz E. 2000. New data on the age of eclogites of the Polar Urals. *Dokl. Earth Sci.* 371:519–23 (in Russian)
- Shervais JW. 2001. Birth, death, and resurrection: the life cycle of suprasubduction zone ophiolites. *Geochem. Geophys. Geosyst.* 2:2000GC000080
- Shervais JW. 2008. Tonalites, trondhjemites, and diorites of the Elder Creek ophiolite, California: low-pressure slab melting and reaction with the mantle wedge. *Geol. Soc. Am. Spec. Pap.* 438:113–32
- Shi GH, Cui WY, Cao SM, Jiang N, Jian P, et al. 2008. Ion microprobe zircon U–Pb age and geochemistry of the Myanmar jadeitite. *J. Geol. Soc.* 165:221–34

- Shi GH, Cui WY, Tropper P, Wang CQ, Shu GM, Yu HX. 2003. The petrology of a complex sodic and sodic-calcic amphibole association and its implications for the metasomatic processes in the jadeitite area in northwestern Myanmar, formerly Burma. *Contrib. Mineral. Petrol.* 145:355–76
- Shi GH, Tropper P, Cui W, Tan J, Wang C. 2005. Methane (CH₄)-bearing fluid inclusions in the Myanmar jadeitite. *Geochem. J.* 39:503–16
- Shigeno M, Mori Y, Nishiyama T. 2005. Reaction microtextures in jadeitites from the Nishisonogi metamorphic rocks, Kyushu, Japan. *J. Mineral. Petrol.* 100:237–46
- Shigeno M, Mori Y, Shimada K, Nishiyama T. 2012. Jadeitites with retrograde metasomatic zoning from the Nishisonogi metamorphic rocks, western Japan: fluid–tectonic block interaction during exhumation. *Eur. J. Mineral.* 24:289–311
- Shoji T, Kobayashi S. 1988. Fluid inclusions found in jadeite and stronalsite, and a comment on the jadeite-analcime boundary. *J. Mineral. Petrol. Econ. Geol.* 83:1–8
- Simons KK, Harlow GE, Sorensen SS, Brueckner HK, Goldstein SL, et al. 2010. Lithium isotopes in Guatemala and Franciscan HP-LT rocks: insights into the role of sediment-derived fluids in the mantle wedge. *Geochim. Cosmochim. Acta* 74:3621–41
- Sisson VB, Sorensen SS, Harlow GE. 2006. Subduction zone fluid composition estimated from fluid inclusions in Guatemalan jadeitite. *Geol. Soc. Am. Abstr. Programs* 38(7):270
- Sobolev VS. 1949. *The Introduction into Silicates Mineralogy*. Lvov, Ukr.: Lvov Univ. Publ. (in Russian)
- Sobolev VS. 1951. On the terms of the alkaline pyroxene and alkaline amphibole. *Mineral. Collect. Lvov Geol. Soc.* 5:316–18 (in Russian)
- Sorensen SS, Barton MD. 1987. Metasomatism and partial melting in a subduction complex: Catalina Schist, southern California. *Geology* 15:115–18
- Sorensen SS, Harlow GE, Rumble D. 2006. The origin of jadeitite-forming subduction zone fluids: CL-guided SIMS oxygen isotope and trace element evidence. *Am. Mineral.* 91:979–96
- Sorensen SS, Sisson VB, Harlow GE, Avé Lallemand HG. 2010. Element residence and transport during subduction zone metasomatism: evidence from a jadeitite-serpentinite contact, Guatemala. *Int. Geol. Rev.* 52:899–940
- Stern RJ, Tsujimori T, Harlow GE, Groat LA. 2013. Plate tectonic gemstones. *Geology* 41:723–26
- Sun SS, McDonough WF. 1989. Chemical and isotopic systematics of oceanic basalts: implications for mantle composition and processes. *Geol. Soc. Spec. Publ.* 42:313–45
- Sun SS, McDonough WF. 1995. The composition of the Earth. *Chem. Geol.* 120:223–53
- Syracuse EM, van Keken PE, Abers GA. 2010. The global range of subduction zone thermal models. *Phys. Earth Planet. Inter.* 183:73–90
- Tsujimori T, Ernst WG. 2014. Lawsonite blueschists and lawsonite eclogites as proxies for paleosubduction zone processes: a review. *J. Metamorph. Geol.* 32:437–54
- Tsujimori T, Harlow GE. 2012. Petrogenetic relationships between jadeitite and associated high-pressure and low-temperature metamorphic rocks in worldwide jadeitite localities: a review. *Eur. J. Mineral.* 24:371–90
- Tsujimori T, Liou JG, Wooden J, Miyamoto T. 2005. U-Pb dating of large zircons in low-temperature jadeitite from the Osayama serpentinite mélange, Southwest Japan: insights into the timing of serpentinization. *Int. Geol. Rev.* 47:1048–57
- Tsujimori T, Sisson VB, Liou JG, Harlow GE, Sorensen SS. 2006a. Petrologic characterization of Guatemalan lawsonite eclogite: eclogitization of subducted oceanic crust in a cold subduction zone. *Geol. Soc. Am. Spec. Pap.* 403:147–68
- Tsujimori T, Sisson VB, Liou JG, Harlow GE, Sorensen SS. 2006b. Very low-temperature record in subduction process: a review of worldwide lawsonite eclogites. *Lithos* 92:609–24
- Wada I, Wang K, He J, Hyndman RD. 2008. Weakening of the subduction interface and its effects on surface heat flow, slab dehydration, and mantle wedge serpentinization. *J. Geophys. Res.* 113:B04402
- Watson KD, Morton DM. 1969. Eclogite inclusions in kimberlite pipes at Garnet Ridge, northeastern Arizona. *Am. Mineral.* 54:267–85
- Whitney DL, Evans BW. 2010. Abbreviations for names of rock-forming minerals. *Am. Mineral.* 95:185–87
- Wohlens A, Manning CE, Thompson AB. 2011. Experimental investigation of the solubility of albite and jadeite in H₂O, with paragonite + quartz at 500 and 600°C and 1–2.25 GPa. *Geochim. Cosmochim. Acta* 75:2924–39

- Yoder HS Jr. 1950. The jadeite problem, parts I and II. *Am. J. Sci.* 248:225–48, 312–34
- Yui TF, Fukuyama M, Iizuka Y, Wu CM, Wu TW, et al. 2013. Is Myanmar jadeitite of Jurassic age? A result from incompletely recrystallized inherited zircon. *Lithos* 160–61:268–82
- Yui TF, Maki K, Usuki T, Lan CY, Martens U, et al. 2010. Genesis of Guatemala jadeitite and related fluid characteristics: insight from zircon. *Chem. Geol.* 270:45–55
- Yui TF, Maki K, Wang KL, Lan CY, Iizuka Y, et al. 2012. Hf isotope and REE compositions of zircon from jadeitite (Tone, Japan and north of the Motagua fault, Guatemala): implications on jadeitite genesis and possible protoliths. *Eur. J. Mineral.* 24:263–75